



CMS-SUS-12-002

CERN-PH-EP/2012-186
2024/11/27

Search for supersymmetry in hadronic final states using $M_{\mathrm{T}2}$ in pp collisions at $\sqrt{s} = 7 \text{ TeV}$

The CMS Collaboration^{*}

Abstract

A search for supersymmetry or other new physics resulting in similar final states is presented using a data sample of 4.73 fb^{-1} of pp collisions collected at $\sqrt{s} = 7 \text{ TeV}$ with the CMS detector at the LHC. Fully hadronic final states are selected based on the variable $M_{\mathrm{T}2}$, an extension of the transverse mass in events with two invisible particles. Two complementary studies are performed. The first targets the region of parameter space with medium to high squark and gluino masses, in which the signal can be separated from the standard model backgrounds by a tight requirement on $M_{\mathrm{T}2}$. The second is optimized to be sensitive to events with a light gluino and heavy squarks. In this case, the $M_{\mathrm{T}2}$ requirement is relaxed, but a higher jet multiplicity and at least one b-tagged jet are required. No significant excess of events over the standard model expectations is observed. Exclusion limits are derived for the parameter space of the constrained minimal supersymmetric extension of the standard model, as well as on a variety of simplified model spectra.

Submitted to the Journal of High Energy Physics

^{*}See Appendix A for the list of collaboration members

1 Introduction

A broad class of extensions of the standard model (SM) predict the existence of heavy colored particles that decay to hadronic final states accompanied by large missing transverse energy (E_T^{miss}). The best known of these scenarios is supersymmetry [1] (SUSY) with R-parity conservation. In this paper we present a search for such new physics in pp collisions collected with the Compact Muon Solenoid (CMS) detector at the Large Hadron Collider (LHC) at a center-of-mass energy of 7 TeV. The results are based on the data sample collected in 2011, corresponding to about 4.73 fb^{-1} of integrated luminosity.

The search makes use of the “transverse mass” variable M_{T2} [2, 3] to select new physics candidate events. M_{T2} is the natural extension of the transverse mass M_{T} to the case where two colored supersymmetric particles (“sparticles”) are pair-produced and both decay through a cascade of jets and possibly leptons to the lightest supersymmetric particle (LSP). The LSP is not visible in the detector and leads to a missing transverse momentum signature. Although M_{T2} was originally introduced to derive the masses of sparticles involved in the cascade decay, we use it here as a discovery variable since it is sensitive to the presence of SUSY-like new physics. The distribution of M_{T2} reflects the produced particle masses, which are much lighter for the SM background processes than for the SUSY processes. Hence, new physics is expected to appear as an excess in the tail of M_{T2} .

The analysis is based on two complementary approaches. A first approach, the “ M_{T2} analysis”, targets events resulting from heavy sparticle production, characterized by large E_T^{miss} , at least three jets, and large M_{T2} . The SM backgrounds in the signal region consist of $W(\ell\nu)$ +jets, $Z(\nu\bar{\nu})$ +jets, $t\bar{t}$, and single-top events (the last two will be referred to collectively as top-quark background), which are estimated from data-control regions and simulation. This analysis loses sensitivity if the squarks are heavy and the gluinos light, in which case the production is dominated by gluino-gluino processes. The gluinos give rise to three-body decays with relatively small E_T^{miss} . Since the gluino decay is mediated by virtual squark exchange and the stop and sbottom are expected to be lighter than the first- and second-generation squarks, these events can be rich in b quarks. To increase the sensitivity to such processes, a second approach, the “ $M_{\text{T2}}b$ analysis”, is developed, in which the threshold on M_{T2} defining the signal region is lowered. To suppress the QCD multijet background, we demand at least one b-tagged jet and place a stricter requirement on the jet multiplicity. The $M_{\text{T2}}b$ analysis provides a larger signal-to-background ratio in the region of heavy squarks and light gluinos and hence improves our sensitivity to this scenario.

This paper extends previous results of searches in fully hadronic final states from the CMS [4–7] and ATLAS [8–11] Collaborations. It is organized as follows: after a brief introduction to M_{T2} and its salient properties in Section 2, and a description of the CMS detector in Section 3, we present in Section 4 the data samples used and the event selection. In Section 5, the search strategy is presented. This strategy is applied to the M_{T2} analysis in Section 6 and to the $M_{\text{T2}}b$ analysis in Section 7. In these sections the background estimation methods are also discussed. We interpret the results in Section 8 in the context of the constrained minimal supersymmetric standard model (CMSSM) as well as for a variety of simplified models. Finally, Section 9 contains a summary.

2 Definition of M_{T2}

The variable M_{T2} was introduced [2] to measure the mass of primary pair-produced particles in a situation where both ultimately decay into undetected particles (e.g., LSPs) leaving the

event kinematics underconstrained. It assumes that the two produced sparticles give rise to identical types of decay chains with two visible systems defined by their transverse momenta $\vec{p}_T^{\text{vis}(i)}$, transverse energies $E_T^{\text{vis}(i)}$, and masses $m^{\text{vis}(i)}$. They are accompanied by the unknown LSP transverse momenta $\vec{p}_T^{\tilde{\chi}(i)}$. In analogy with the transverse mass used for the W boson mass determination [12], we can define two transverse masses ($i = 1, 2$):

$$(M_T^{(i)})^2 = (m^{\text{vis}(i)})^2 + m_{\tilde{\chi}}^2 + 2 \left(E_T^{\text{vis}(i)} E_T^{\tilde{\chi}(i)} - \vec{p}_T^{\text{vis}(i)} \cdot \vec{p}_T^{\tilde{\chi}(i)} \right). \quad (1)$$

These have the property (as in W-boson decays) that, for the true LSP mass $m_{\tilde{\chi}}$, their distribution cannot exceed the mass of the parent particle of the decay and they present an endpoint at the value of the parent mass. The momenta $\vec{p}_T^{\tilde{\chi}(i)}$ of the invisible particles are not experimentally accessible individually. Only their sum, the missing transverse momentum \vec{p}_T^{miss} , is known. Therefore, in the context of SUSY, a generalization of the transverse mass is needed and the proposed variable is M_{T2} . It is defined as

$$M_{T2}(m_{\tilde{\chi}}) = \min_{\vec{p}_T^{\tilde{\chi}(1)} + \vec{p}_T^{\tilde{\chi}(2)} = \vec{p}_T^{\text{miss}}} \left[\max \left(M_T^{(1)}, M_T^{(2)} \right) \right], \quad (2)$$

where the LSP mass $m_{\tilde{\chi}}$ remains a free parameter. This formula can be understood as follows. As neither $M_T^{(1)}$ nor $M_T^{(2)}$ can exceed the parent mass if the true momenta are used, the larger of the two can be chosen. To make sure that M_{T2} does not exceed the parent mass, a minimization is performed on trial LSP momenta fulfilling the \vec{p}_T^{miss} constraint. The distribution of M_{T2} for the correct value of $m_{\tilde{\chi}}$ then has an endpoint at the value of the primary particle mass. If, however, $m_{\tilde{\chi}}$ is lower (higher) than the correct mass value, the endpoint will be below (above) the parent mass. An analytic expression for M_{T2} has been computed [13] assuming that initial-state radiation (ISR) can be neglected. In practice, the determination of M_{T2} may be complicated by the presence of ISR or, equivalently, transverse momentum arising from decays that occur upstream in the decay chain [14]. In this case, no analytic expression for M_{T2} is known, but it can be computed numerically, using, e.g., the results of Ref. [15].

To illustrate the behavior of M_{T2} , we consider the simple example of M_{T2} without ISR or upstream transverse momentum. As discussed in Ref. [13], the angular and p_T dependence of M_{T2} is encoded in a variable A_T :

$$A_T = E_T^{\text{vis}(1)} E_T^{\text{vis}(2)} + \vec{p}_T^{\text{vis}(1)} \cdot \vec{p}_T^{\text{vis}(2)}, \quad (3)$$

and M_{T2} increases as A_T increases. Therefore, the minimum value of M_{T2} is reached in configurations where the visible systems are back-to-back. The maximum value is reached when they are parallel to each other and have large p_T . In the simple case where $m_{\tilde{\chi}} = 0$ and the visible systems have zero mass, M_{T2} becomes

$$(M_{T2})^2 = 2A_T = 2p_T^{\text{vis}(1)} p_T^{\text{vis}(2)} (1 + \cos \phi_{12}), \quad (4)$$

where ϕ_{12} is the angle between the two visible systems in the transverse plane. It can be seen that Eq. (4) corresponds to the transverse mass of two systems $(M_T)^2 = 2p_T^{\text{sys}(1)} p_T^{\text{sys}(2)} (1 - \cos \phi_{12})$, with $\vec{p}_T^{\text{vis}} = -\vec{p}_T^{\text{sys}}$ for one of the systems.

In this paper, we use M_{T2} as a variable to distinguish potential new physics events from SM backgrounds. The use of M_{T2} as a discovery variable was first proposed in Ref. [16], but here we follow a different approach. Several choices for the visible system used as input to M_{T2} can be considered: dijet events (as in Ref. [16]), the two jets with largest p_T in multijet events,

or two systems of pseudojets defined by grouping jets together. In this study, we use the last method.

A technique to group jets in multijet events into two pseudojets is the “event hemispheres” method described in Ref. [17] (see Section 13.4). We take the two initial axes as the directions of the two massless jets that yield the largest dijet invariant mass. The pseudojets are then formed based on a minimization of the Lund distance criterion [17, 18].

We use $M_{\mathrm{T}2}$ as our main search variable since SUSY events with large expected $E_{\mathrm{T}}^{\mathrm{miss}}$ and jet acoplanarity will be concentrated in the large $M_{\mathrm{T}2}$ region. In contrast, QCD dijet events, in which the two jets are back-to-back, populate the region of small $M_{\mathrm{T}2}$ regardless of the value of $E_{\mathrm{T}}^{\mathrm{miss}}$ or jet p_{T} . In the present study, we choose the visible systems to be massless and set $m_{\tilde{\chi}} = 0$. Then back-to-back dijet events will have $M_{\mathrm{T}2} = 0$, as explained above. Hence, $M_{\mathrm{T}2}$ has a built-in protection against jet mismeasurements in QCD dijet events, even if accompanied by large $E_{\mathrm{T}}^{\mathrm{miss}}$. However, QCD multijet events with large $E_{\mathrm{T}}^{\mathrm{miss}}$ may give rise to acoplanar pseudojets, leading to larger $M_{\mathrm{T}2}$ values. For this reason, further protections against $E_{\mathrm{T}}^{\mathrm{miss}}$ from mismeasurements need to be introduced, as described below. Other SM backgrounds, such as $t\bar{t}$, single top-quark, and $W+\mathrm{jets}$ events with leptonic decays, or $Z+\mathrm{jets}$ events where the Z boson decays to neutrinos, contain true $E_{\mathrm{T}}^{\mathrm{miss}}$ and can also lead to acoplanar pseudojets.

3 CMS detector

The central feature of the CMS apparatus is a superconducting solenoid 13 m in length and 6 m in diameter that provides an axial magnetic field of 3.8 T. The core of the solenoid is instrumented with various particle detection systems: a silicon pixel and strip tracker, an electromagnetic calorimeter (ECAL), and a brass/scintillator hadron calorimeter (HCAL). The silicon pixel and strip tracker covers $|\eta| < 2.5$, where pseudorapidity η is defined by $\eta = -\ln [\tan(\theta/2)]$ with θ the polar angle of the trajectory of the particle with respect to the counterclockwise beam direction. The ECAL and HCAL cover $|\eta| < 3$. The steel return yoke outside the solenoid is instrumented with gas detectors used to identify muons. A quartz-steel Cerenkov-radiation-based forward hadron calorimeter extends the coverage to $|\eta| \leq 5$. The detector is nearly hermetic, covering $0 < \phi < 2\pi$ in azimuth, allowing for energy balance measurements in the plane transverse to the beam directions. The first level of the CMS trigger system, composed of custom hardware processors, uses information from the calorimeters and muon detectors to select the most interesting events in a fixed time interval of less than 4 μs . The High Level Trigger processor farm further decreases the event rate from around 100 kHz to around 300 Hz, before data storage. A detailed description of the CMS detector can be found elsewhere [19].

4 Samples and event selection

The data used in this analysis were collected by triggers based on the quantity H_{T} , the scalar sum of transverse momenta of reconstructed and energy-corrected calorimeter jets. Due to a continuous increase in the instantaneous luminosity of the LHC, the trigger evolved with time from the requirement $H_{\mathrm{T}} > 440 \text{ GeV}$ to $H_{\mathrm{T}} > 750 \text{ GeV}$. In this analysis, only triggers with a threshold of 650 GeV or less have been used, corresponding to a total integrated luminosity of 4.73 fb^{-1} .

The analysis is designed using simulated event samples created with the PYTHIA 6.4.22 [18] and MADGRAPH 5v1.1 [20] Monte Carlo event generators. These events are subsequently processed with a detailed simulation of the CMS detector response based on GEANT4 [21]. The events are

reconstructed and analyzed in the same way as the data. The SUSY signal particle spectrum is calculated using SOFTSUSY [22] and for the decays SDECAY [23] is used. We use two CMS SUSY benchmark signal samples, referred to as LM6 and LM9 [17], to illustrate possible CMSSM [24] yields. The CMSSM is defined by the universal scalar and gaugino mass parameters m_0 and $m_{1/2}$, respectively, the parameter A_0 of the trilinear couplings, the ratio of the vacuum expectation values of the two Higgs fields $\tan \beta$, and the sign of the Higgs mixing parameter sign (μ). The parameter values for LM6 are $m_0 = 85\text{ GeV}$, $m_{1/2} = 400\text{ GeV}$, $\tan \beta = 10$, $A_0 = 0\text{ GeV}$ and $\text{sign}(\mu) > 0$. Those for LM9 are $m_0 = 1450\text{ GeV}$, $m_{1/2} = 175\text{ GeV}$, $\tan \beta = 50$, $A_0 = 0\text{ GeV}$ and $\text{sign}(\mu) > 0$. All samples are generated using the CTEQ6 [25] parton distribution functions (PDFs). For SM background simulated samples we use the most accurate calculation of the cross sections currently available, usually with next-to-leading-order (NLO) accuracy. For the CMS SUSY benchmark signal samples we use NLO cross sections of 0.403 pb and 10.6 pb for LM6 and LM9, respectively, obtained by weighting the leading order cross sections from PYTHIA with sub-process dependent K-factors calculated with PROSPINO [26].

The events are reconstructed using the particle-flow (PF) algorithm [27], which identifies and reconstructs individually the particles produced in the collision, namely charged hadrons, photons, neutral hadrons, electrons, and muons.

Electrons and muons with $p_T \geq 10\text{ GeV}$ and $|\eta| \leq 2.4$ are considered isolated if the transverse momentum sum of charged hadrons, photons, and neutral hadrons surrounding the lepton within a cone of radius $\sqrt{(\Delta\eta)^2 + (\Delta\phi)^2} = 0.4$, divided by the lepton transverse momentum value itself, is less than 0.2. The electron and muon reconstruction and identification algorithms are described in Refs. [28, 29] and [30], respectively. All particles apart from the isolated electrons and muons are clustered into jets using the anti- k_T jet clustering algorithm [31] with distance parameter 0.5 [32, 33]. Jet energies are calibrated by applying correction factors as a function of the transverse momentum and the pseudorapidity of the jet. Residual jet energy corrections are applied to jets in data to account for differences in jet energy scale between simulation and data [34]. The effect of pileup, namely multiple pp collisions within a beam crossing, is reduced by using the FastJet pileup subtraction procedure [35, 36] for data and simulated events. Jets are required to pass loose identification criteria and to satisfy $p_T > 20\text{ GeV}$ and $|\eta| \leq 2.4$. The b-jet tagging is based on the simple-secondary-vertex algorithm [37]. We use the high-purity working point that yields a typical jet-tagging efficiency of 42% for b jets in our search region while the mistagging efficiency for light-flavored (uds quark and gluon) jets is of the order of 0.1% and for c jets, 6.3%. The missing transverse momentum \vec{E}_T^{miss} is computed as the negative vector sum of all particles reconstructed by the PF algorithm [33].

Events are required to contain at least one good primary vertex [38]. The H_T value, computed from PF jets with $p_T > 50\text{ GeV}$, must satisfy $H_T \geq 750\text{ GeV}$. With this H_T requirement, the triggers are nearly 100% efficient. At least three jets are required, where a p_T threshold of 40 GeV is used for jet counting. The two leading jets are required to have $p_T > 100\text{ GeV}$. The value of E_T^{miss} is required to exceed 30 GeV . Events containing beam background or anomalous calorimeter noise are rejected. To reject events where a significant fraction of the momentum imbalance arises from forward or soft jets, a maximum difference of 70 GeV is imposed on the modulus of the difference between the \vec{E}_T^{miss} and \vec{H}_T^{miss} vectors, where \vec{H}_T^{miss} is the negative vector sum of all selected jets. Events containing jet candidates with $p_T > 50\text{ GeV}$ that fail the jet identification criteria are also rejected.

To reduce the background from QCD multijet events with large E_T^{miss} , arising from mismeasurements or leptonic heavy flavor decays, a minimum azimuthal difference $\Delta\phi_{\min}(\text{jets}, \vec{E}_T^{\text{miss}}) > 0.3$ is required between the directions of \vec{E}_T^{miss} and any jet with $p_T > 20\text{ GeV}$. Finally, events

are rejected if they contain an isolated electron or muon, to suppress the contributions from W+jets, Z+jets and top-quark backgrounds.

5 Search strategy

The M_{T2} variable is computed after applying the selection criteria of Section 4. We separately consider fully hadronic channels with ≥ 3 jets and a tight M_{T2} requirement (the M_{T2} analysis), which is mostly sensitive to signal regions with large squark and gluino masses, and channels with ≥ 4 jets, at least one tagged b jet, and a relaxed M_{T2} requirement (the $M_{T2}b$ analysis), which increases sensitivity to regions with small gluino and large squark masses.

Given the event selection outlined above, we do not expect a significant number of QCD multijet events to appear in the signal regions. Nonetheless, we estimate an upper limit on the remaining QCD multijet background in the signal regions from data control samples. The main backgrounds, consisting of W+jets, Z+jets, and top-quark production, are evaluated from data control samples and simulation. A common strategy is applied to both the M_{T2} and $M_{T2}b$ analyses:

- Two regions are defined in H_T , a low H_T region $750 \leq H_T < 950$ GeV and a high H_T region $H_T \geq 950$ GeV. In each region, several adjacent bins in M_{T2} are defined: five bins for the M_{T2} analysis and four for the $M_{T2}b$ analysis. The lowest bin in M_{T2} is chosen such that the expected QCD multijet background remains a small fraction of the total background. For the M_{T2} analysis the lowest bin starts at $M_{T2} = 150$ GeV and for $M_{T2}b$ at $M_{T2} = 125$ GeV.
- A dedicated method for each background is designed to estimate its contribution in the signal region from data control samples and simulation. The number of events and their relative systematic uncertainties are computed by means of these methods in each H_T , M_{T2} bin. The methods are designed such that the resulting estimates are largely uncorrelated statistically.
- The predicted number of events for all background components and their uncertainties are combined, resulting in an estimate of the total background yield and its uncertainty in each bin.
- The estimated number of background events for each bin is compared to the number of observed events, and the potential contribution from a SUSY signal is quantified by a statistical method described in Section 8.

6 M_{T2} analysis

Figure 1 shows the measured M_{T2} distribution in comparison to simulation. For $M_{T2} < 80$ GeV the distribution is completely dominated by QCD multijet events. For medium M_{T2} values, the distribution is dominated by W+jets and $Z(\nu\bar{\nu})$ +jets events with some contribution from top-quark events, while in the tail of M_{T2} the contribution from top-quark production becomes negligible and $Z(\nu\bar{\nu})$ +jets together with W+jets events dominate. We observe good agreement between data and simulation in the core as well as in the tail of the distribution. The white histogram (black dotted line) corresponds to the LM6 signal. It can be noted that in the presence of signal, an excess in the tail of M_{T2} is expected.

The corresponding event yields for data and SM simulated samples, after the full selection and for the various bins in M_{T2} , are given in Table 1 for the low and the high H_T regions.

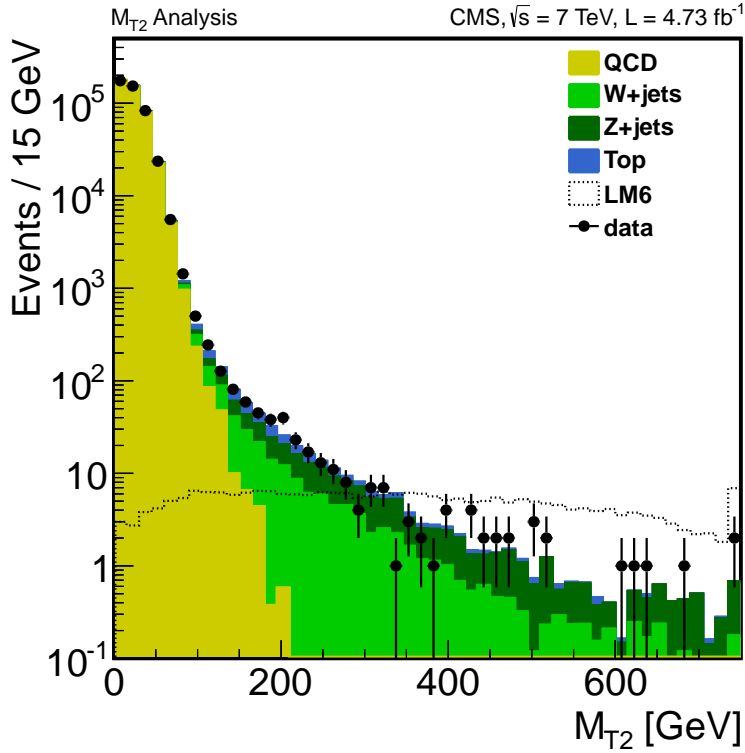


Figure 1: The M_{T2} distribution with all selection requirements applied and $H_T \geq 750$ GeV. The different predictions for the SM backgrounds from simulation are stacked on top of each other. The LM6 signal distribution is not stacked. All distributions from simulation are normalized to the integrated luminosity of the data.

Table 1: Observed number of events and expected SM background yields from simulation in M_{T2} bins for the low and high H_T regions. These numbers are for guidance only and are not used in the final background prediction.

	QCD multijet	$W+jets$	Top	$Z(\nu\nu)+jets$	Total SM	Data
$750 \leq H_T < 950$						
$M_{T2}[0, \infty]$	3.18e+05	9.22e+02	1.30e+03	3.01e+02	3.20e+05	3.20e+05
$M_{T2}[150, 200]$	3.08	37.5	20.6	27.9	90.0	88
$M_{T2}[200, 275]$	0.0	20.6	9.40	20.3	50.3	69
$M_{T2}[275, 375]$	0.0	9.74	2.74	11.6	24.1	19
$M_{T2}[375, 500]$	0.0	3.63	0.69	6.07	10.4	8
$M_{T2}[500, \infty]$	0.0	1.54	0.20	3.55	5.29	6
$H_T \geq 950$						
$M_{T2}[0, \infty]$	1.22e+05	4.39e+02	6.32e+02	1.42e+02	1.23e+05	1.19e+05
$M_{T2}[150, 200]$	9.84	19.8	11.7	12.9	54.2	70
$M_{T2}[200, 275]$	0.47	13.7	5.25	10.5	30.0	23
$M_{T2}[275, 375]$	0.04	6.43	1.83	6.42	14.7	9
$M_{T2}[375, 500]$	0.0	1.63	0.40	2.54	4.57	8
$M_{T2}[500, \infty]$	0.0	1.10	0.16	2.16	3.42	4

Contributions from other backgrounds, such as γ +jets, $Z(\ell\ell)$ +jets and diboson production, are found to be negligible. It is seen that for all but one M_{T2} bin, the observed number of events agrees within the uncertainties with the SM background expectation from simulation. In the low H_T region, the M_{T2} bin [200, 275] GeV exhibits an excess in data compared to background. We investigated whether the origin could be instrumental in nature, but did not find evidence for it. It could be of statistical origin. The excess has a marginal impact on the final observed limit.

6.1 Background prediction

6.1.1 QCD multijet background

The simulation predicts that the QCD multijet background is negligible in the tail of the M_{T2} distribution. Nevertheless, a dedicated method using a data control region was designed to verify that this is indeed the case.

We base this estimation on M_{T2} and $\Delta\phi_{\min}$, which is the difference in azimuth between \vec{E}_T^{miss} and the closest jet. The background in the signal region, defined by $\Delta\phi_{\min} \geq 0.3$ and large M_{T2} , is predicted from a control region with $\Delta\phi_{\min} \leq 0.2$. The two variables are strongly correlated, but a factorization method can still be applied if the functional form is known for the ratio of the number of events $r(M_{T2}) = N(\Delta\phi_{\min} \geq 0.3)/N(\Delta\phi_{\min} \leq 0.2)$ as a function of M_{T2} . It is found from simulation studies, and confirmed with data, that for $M_{T2} > 50$ GeV the ratio falls exponentially. Therefore, a parameterization of the form

$$r(M_{T2}) = \frac{N(\Delta\phi_{\min} \geq 0.3)}{N(\Delta\phi_{\min} \leq 0.2)} = \exp(a - bM_{T2}) + c \quad (5)$$

is used for $M_{T2} > 50$ GeV. The function is assumed to reach a constant value at large M_{T2} due to extreme tails of the jet energy resolution response.

The method is validated with simulation. First the parameters a , b , and c are extracted from a fit to simulated QCD multijet events in the full M_{T2} spectrum. The fitted parameter value for c is compatible with a negligible QCD multijet contribution at large M_{T2} . It is verified that similar fit results for the parameters a and b are obtained when the fit is limited to the region $50 < M_{T2} < 80$ GeV, where contributions from background processes other than that from QCD multijets is small. The robustness of the prediction is checked by systematically varying the fit boundaries.

For the final results, we repeat the fit to data in the region $50 < M_{T2} < 80$ GeV, after subtracting the W +jets, Z +jets and top background contributions using simulation. The fitted parameter values for a and b are in agreement with the values obtained from the QCD multijet simulation. We conservatively fix the constant c to the value of the exponential at $M_{T2} = 250$ GeV, where agreement with data can still be verified. In the lower M_{T2} bins, where the exponential term dominates, the method reliably predicts the QCD multijet background. For higher M_{T2} bins, where the constant term dominates, the method overestimates the number of QCD multijet events relative to the simulation, nonetheless confirming that the QCD multijet contribution is negligible.

The extreme case of total loss of a jet, leading to population of the high M_{T2} tail, is studied using a sample of high p_T mono-jet events obtained with a dedicated event selection. The total number of events is found to be compatible within the uncertainties with the number expected from the electroweak processes, confirming that the QCD multijet contribution is negligible and hence that the constant c is small.

6.1.2 $W(\ell\nu)$ +jets and top-quark background

The backgrounds due to $W(\ell\nu)$ +jets and to semi-leptonic decays of top quarks have the following sources in common:

- leptonic decays of the W boson, where the lepton is unobserved because it falls outside the p_T or η acceptance;
- to a lesser extent, leptonic decays of the W boson, where the lepton is within the acceptance but fails to satisfy the reconstruction, identification, or isolation criteria;
- $W(\tau\nu_\tau)$ decays, where the τ decays hadronically.

We refer to leptons that fall into either of the first two categories as “lost leptons”. The number of events with lost leptons is estimated from a data control sample where a single lepton (e or μ) is found. A correction factor accounting for the probability to lose the lepton is derived from simulation. To avoid a potential contamination from signal events, a transverse mass cut $M_T < 100\text{ GeV}$ is introduced. This method is applied in the various H_T and M_{T2} bins. First, a successful validation test of the method is performed using simulated samples. Then, a prediction is made from the data bin by bin and found to be in agreement with the expectation from simulation. A systematic uncertainty is evaluated that includes the uncertainty on the lepton efficiencies, acceptance, and background subtraction.

For the background contribution from hadronically decaying tau leptons, a method similar to the one described above is used. Events with an isolated and identified hadronically decaying tau [39] lepton are selected in the various H_T and M_{T2} bins. The contribution from jets misidentified as taus is subtracted. The remaining number of tau events is corrected for the tau reconstruction and identification efficiency. The predicted number of hadronically decaying tau background events agrees with the true number from simulation. Given the small number of events in the data, the numbers of events from the simulation are used for the background estimate, with the same relative systematic uncertainties as for the lost leptons.

6.1.3 $Z(\nu\bar{\nu})$ +jets background

The estimate of the $Z(\nu\bar{\nu})$ +jets background is obtained independently from two distinct data samples, one containing γ +jets events and the other $W(\mu\nu)$ +jets events. In both cases the invisible decay of the Z boson is mimicked by removing, respectively, the photon and the muon from the event, and adding vectorially the corresponding \vec{p}_T to \vec{E}_T^{miss} .

For the estimate based on γ +jets events, a sample of events with identified and isolated photons [40] with $p_T > 20\text{ GeV}$ is selected, where all selection requirements except that on M_{T2} are imposed. This sample contains both prompt photons and photons from π^0 decays in QCD multijet events. The two components are separated by performing a maximum likelihood fit of templates from simulated events to the shower shapes. The event sample is dominated by low p_T photons, where the shower shape provides high discrimination power between prompt photons and π^0 s. The extrapolation of their contributions as a function of M_{T2} is obtained from simulation. The $Z(\nu\bar{\nu})$ +jets background is estimated for each bin in M_{T2} from the number of prompt photon events multiplied by the M_{T2} -dependent ratio of $Z(\nu\bar{\nu})$ +jets to γ +jets events obtained from simulation. This ratio increases as a function of the photon p_T (which drives the M_{T2} value) and reaches a constant value above 300 GeV . The resulting prediction of the background is found to be in good agreement with the expectation from simulation. Systematic uncertainties on the background prediction consist of the statistical uncertainties from the number of γ +jets events, a normalization uncertainty in the shower shape fit of 5%, and the systematic uncertainties on the ratio of $Z(\nu\bar{\nu})$ +jets to γ +jets events in the simulation. The un-

certainties on the ratio are estimated to be less than 20% (30%) for $M_{T2} < 275$ ($M_{T2} > 275$) GeV. To assess these uncertainties, the p_T dependence of the ratio is studied in data and compared to simulation using leptonically decaying Z events. For $p_T > 400$ GeV this test is limited by the number of the leptonic Z events, which justifies the increased uncertainty for $M_{T2} > 275$ GeV.

For the estimate from $W(\mu\nu)$ +jets events, corrections are needed for lepton acceptance, lepton reconstruction efficiency, and the ratio between the production cross sections for W and Z bosons (including differences between the shapes of the distributions on which selection criteria are applied). The lepton efficiencies are taken from studies of $Z(\mu\mu)$ events in data. Also, the top-quark background to the W+jets sample is subtracted. The top-quark background is evaluated by applying b tagging to the data to identify top-quark decays and then correcting for the b-tagging efficiency. The $Z(\nu\bar{\nu})$ +jets background is then estimated in each of the M_{T2} bins. The systematic uncertainty includes the contributions from the lepton selection and reconstruction efficiencies, the b-tagging efficiency, the acceptance from simulation, and the W-to-Z ratio.

The $Z(\nu\bar{\nu})$ +jets background estimates from the γ +jets and $W(\mu\nu)$ +jets methods are in good agreement with each other. Since they are statistically uncorrelated, we take the weighted average of the two predictions as the final estimate.

6.2 Results

The results of the background estimation methods for each background contribution are summarized in Table 2 and shown in Fig. 2.

Table 2: Estimated event yields for each background contribution in the various M_{T2} and H_T bins. The predictions from control regions in data are compared to the expected event yields from simulation. Statistical and systematic uncertainties are added in quadrature. The total background prediction is compared to data in the last two columns.

	$Z \rightarrow \nu\bar{\nu}$		Lost lepton		$\tau \rightarrow \text{had}$	QCD multijet		Total bkg.	Data
	sim.	data pred.	sim.	data pred.	Estimate	sim.	data pred.	data pred.	
$750 \leq H_T < 950$									
$M_{T2}[150, 200]$	27.9	24.2 ± 4.9	36.0	29.6 ± 7.1	22.5 ± 5.4	3.1	7.0 ± 3.5	83.3 ± 10.7	88
$M_{T2}[200, 275]$	20.3	21.8 ± 4.8	17.2	11.9 ± 3.9	12.7 ± 4.2	0.0	1.0 ± 0.5	47.4 ± 7.5	69
$M_{T2}[275, 375]$	11.6	13.7 ± 3.8	7.1	4.2 ± 1.9	5.4 ± 2.5	0.0	0.14 ± 0.07	23.4 ± 4.9	19
$M_{T2}[375, 500]$	6.1	4.1 ± 1.6	2.2	1.1 ± 0.9	2.2 ± 1.8	0.0	0.08 ± 0.05	7.4 ± 2.6	8
$M_{T2}[500, \infty]$	3.5	1.8 ± 0.9	1.1	1.2 ± 1.0	0.6 ± 0.5	0.0	0.00 ± 0.00	3.6 ± 1.4	6
$H_T \geq 950$									
$M_{T2}[150, 200]$	12.9	16.7 ± 3.6	18.7	16.2 ± 5.3	12.7 ± 4.1	9.8	11.0 ± 5.5	56.6 ± 9.4	70
$M_{T2}[200, 275]$	10.5	4.5 ± 2.0	11.7	10.2 ± 3.7	7.1 ± 2.6	0.47	1.4 ± 0.7	23.2 ± 5.0	23
$M_{T2}[275, 375]$	6.4	5.7 ± 2.2	5.0	2.9 ± 1.7	3.3 ± 1.9	0.04	0.13 ± 0.07	12.1 ± 3.3	9
$M_{T2}[375, 500]$	2.5	3.0 ± 1.4	1.1	0.6 ± 0.6	0.9 ± 0.9	0.0	0.06 ± 0.04	4.6 ± 1.8	8
$M_{T2}[500, \infty]$	2.2	2.5 ± 1.5	0.6	0.6 ± 0.6	0.6 ± 0.6	0.0	0.06 ± 0.04	3.8 ± 1.7	4

7 $M_{T2}b$ analysis

The selection criteria developed for the M_{T2} analysis are not optimal for events with heavy squarks and light gluinos, such as are predicted by the SUSY benchmark model LM9. To improve sensitivity to these types of events, we perform the $M_{T2}b$ analysis based on loosened kinematic selection criteria and the requirement of a tagged b jet. The restriction on M_{T2} is loosened to $M_{T2} > 125$ GeV and the $\Delta\phi_{\min}(\text{jets}, \vec{E}_T^{\text{miss}}) > 0.3$ requirement is applied to the four

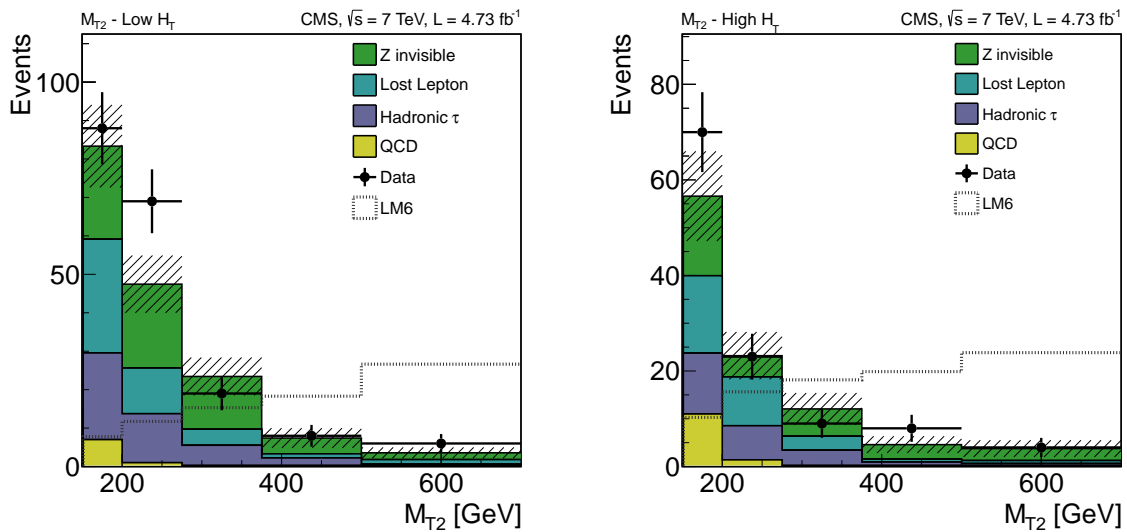


Figure 2: M_{T2} distribution from the background estimates compared to data. The figure on the left corresponds to the $750 \leq H_T < 950$ GeV region, while that on the right corresponds to $H_T \geq 950$ GeV. The predictions from simulated events for the LM6 signal model (not stacked) are also shown. The hatched band shows the total uncertainty on the SM background estimate.

leading jets only. We require that there be at least four jets with $p_T > 40$ GeV, and the leading jet to have $p_T > 150$ GeV. We further require that at least one of the jets in the event be tagged as a b-quark jet.

Figure 3 shows the M_{T2} distribution for events that satisfy the $M_{T2}b$ selection criteria and with $H_T \geq 750$ GeV. As for the M_{T2} analysis (Fig. 1), the QCD multijet background dominates for $M_{T2} < 80$ GeV but is strongly suppressed for $M_{T2} \geq 125$ GeV. In the signal region, top-quark events dominate the electroweak contribution. The white histogram (black dotted line) corresponds to the LM9 signal. The corresponding event yields for data and SM simulation for the low and high H_T regions are summarized in Table 3.

Table 3: Observed number of events and expected SM background event yields from simulation in the various M_{T2} bins for the $M_{T2}b$ event selection. These numbers are for guidance only and are not used in the final background prediction.

	QCD multijet	W+jets	Top	Z($\nu\nu$)+jets	Total SM	Data
$750 \leq H_T < 950$						
$M_{T2}[0, \infty]$	2.83e+04	4.53e+02	1.15e+03	1.41e+02	2.97e+04	2.99e+04
$M_{T2}[125, 150]$	5.16	1.86	20.3	0.95	28.3	22
$M_{T2}[150, 200]$	0.16	1.94	17.9	2.00	22.1	16
$M_{T2}[200, 300]$	0.0	1.84	9.43	1.25	12.6	16
$M_{T2}[300, \infty]$	0.0	0.57	2.55	0.53	3.65	2
$H_T \geq 950$						
$M_{T2}[0, \infty]$	1.19e+04	2.18e+01	5.46e+02	6.51e+00	1.25e+04	1.23e+04
$M_{T2}[125, 150]$	1.25	0.76	9.95	0.64	12.7	10
$M_{T2}[150, 180]$	0.57	0.79	7.15	0.43	8.96	10
$M_{T2}[180, 260]$	0.67	1.09	6.62	0.68	9.06	9
$M_{T2}[260, \infty]$	0.04	0.76	3.09	0.65	4.55	3

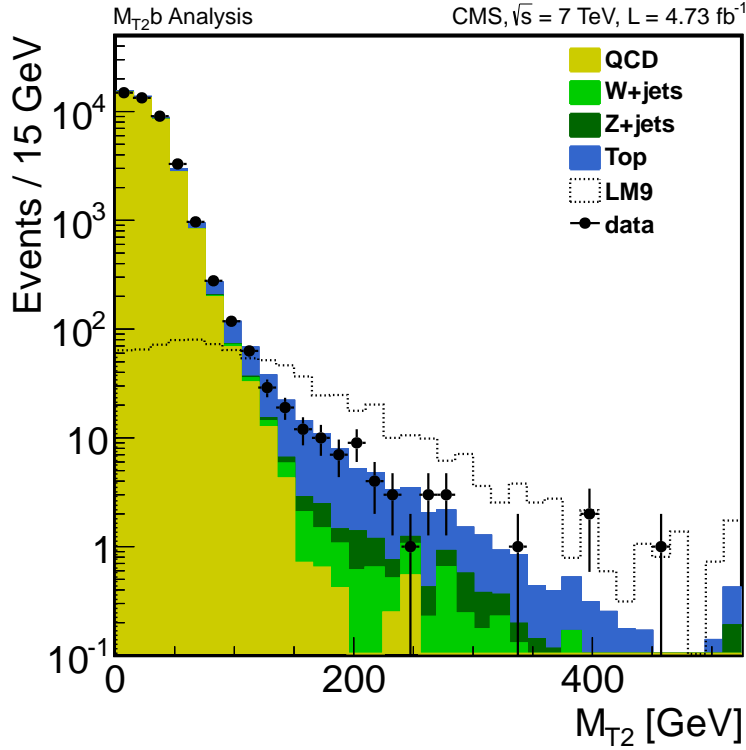


Figure 3: M_{T2} for events with the M_{T2b} selection criteria applied and with $H_T \geq 750\text{ GeV}$. The different predictions from simulation for the SM backgrounds are stacked on top of each other. The LM9 signal distribution is not stacked. All distributions from simulation are normalized to the integrated luminosity of the data.

7.1 Background prediction and results

The QCD multijet contribution is estimated following the same approach as for the M_{T2} analysis. We find that the function in Eq. (5) fitted to data in the region $50 < M_{T2} < 80\text{ GeV}$ provides a good description of the QCD multijet background, also for events containing b-tagged jets. From the fit to data, the prediction of the QCD multijet background is obtained in the various M_{T2} bins for the low and high H_T regions.

Events arising from top-quark production are the dominant background contribution in the signal region. The top-quark contribution is evaluated, together with the one from $W(\ell\nu)+\text{jets}$, in the same way as for the M_{T2} analysis, using single-electron and single-muon events, as well as taus decaying to hadrons.

The background from $Z(\nu\bar{\nu})+\text{jets}$ events is expected to be very small compared with the background from top-quark events. We estimate the background from $Z(\nu\bar{\nu})+\text{jets}$ events with the method based on $W+\text{jets}$ events discussed for the M_{T2} analysis. As the selection of $W(\mu\nu)+\text{jets}$ events includes a b-tag veto to suppress the top-quark background, a ratio of efficiencies for $W(\mu\nu)+\text{jets}$ events with a b tag to $W(\mu\nu)+\text{jets}$ events without a b tag is taken into account. This ratio is obtained from simulation.

The results of the estimates for the various backgrounds are summarized in Table 4 and shown in Fig. 4.

Table 4: Estimated event yields for each background contribution in the various M_{T2} and H_T bins. The predictions from control regions in data are compared to the expected event yields from simulation. Statistical and systematic uncertainties are added in quadrature. The total background prediction is compared to data in the last two columns.

	$Z \rightarrow \nu\bar{\nu}$		Lost lepton		$\tau \rightarrow \text{had}$	QCD multijet		Total bkg.	Data
	sim.	data pred.	sim.	data pred.	Estimate	sim.	data pred.	data pred.	data
$750 \leq H_T < 950$									
$M_{T2}[125, 150]$	1.0	0.5 ± 0.4	12.8	4.5 ± 3.2	8.7 ± 6.3	5.16	4.1 ± 2.1	17.8 ± 7.3	22
$M_{T2}[150, 200]$	2.0	0.7 ± 0.3	11.3	7.6 ± 3.6	8.0 ± 3.8	0.16	0.90 ± 0.51	17.2 ± 5.2	16
$M_{T2}[200, 300]$	1.3	1.0 ± 0.5	6.1	1.3 ± 1.7	4.9 ± 6.7	0.0	0.04 ± 0.03	7.2 ± 6.9	16
$M_{T2}[300, \infty]$	0.5	0.6 ± 0.3	1.3	1.3 ± 0.9	1.8 ± 1.3	0.0	0.00 ± 0.00	3.7 ± 1.6	2
$H_T \geq 950$									
$M_{T2}[125, 150]$	0.6	0.4 ± 0.3	6.2	5.9 ± 3.3	4.3 ± 2.4	1.25	5.4 ± 2.8	16.0 ± 4.9	10
$M_{T2}[150, 180]$	0.4	0.9 ± 0.4	4.6	6.4 ± 3.3	3.2 ± 1.7	0.57	1.7 ± 0.9	12.2 ± 3.9	10
$M_{T2}[180, 260]$	0.6	0.1 ± 0.1	4.2	3.4 ± 2.3	3.3 ± 2.3	0.67	0.45 ± 0.25	7.2 ± 3.2	9
$M_{T2}[260, \infty]$	0.6	0.7 ± 0.4	2.2	2.0 ± 1.6	1.6 ± 1.3	0.04	0.05 ± 0.04	4.3 ± 2.0	3

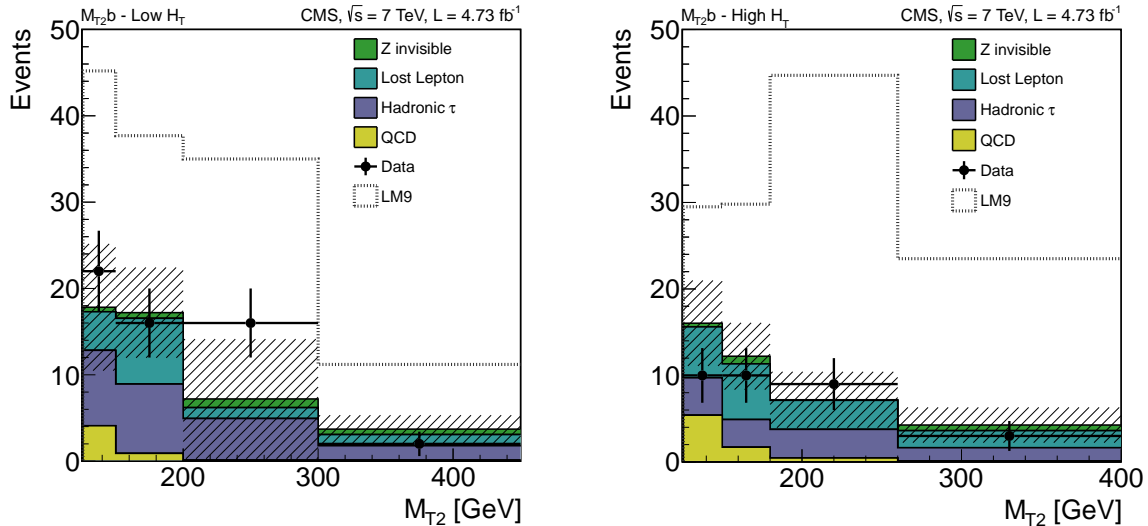


Figure 4: M_{T2} distribution from the background estimates compared to data for the $M_{T2}b$ selection. The figure on the left corresponds to the $750 \leq H_T < 950$ GeV region, while that on the right corresponds to $H_T \geq 950$ GeV. The prediction from simulation for the LM9 signal model (not stacked) are also shown. The hatched band shows the total uncertainty on the SM background estimate.

8 Statistical Interpretation of the results and exclusion limits

No significant deviation from the SM background prediction is observed and upper limits are set on a potential signal. The statistical approach used to derive limits follows closely the methodology of Ref. [41]. A brief description of the steps relevant to this analysis follows.

First, a likelihood function is constructed as the product of Poisson probabilities for each H_T , M_{T2} search bin. These probabilities are functions of the predicted signal and background yields in each bin. Systematic uncertainties are introduced as nuisance parameters in the signal and background models. Log-normal distributions are taken as a suitable choice for the probability density distributions for the nuisance parameters.

In order to compare the compatibility of the data with the background-only and the signal-plus-background hypotheses, we construct the test statistic q_λ based on the profile likelihood ratio:

$$q_\lambda = -2 \ln \frac{\mathcal{L}(\text{data}|\lambda, \hat{\theta}_\lambda)}{\mathcal{L}(\text{data}|\hat{\lambda}, \hat{\theta})}, \quad \text{with } 0 \leq \hat{\lambda} \leq \lambda, \quad (6)$$

where the signal strength modifier λ is introduced to test signal cross section values $\sigma = \lambda \sigma_{\text{sig}}$. Both the denominator and the numerator are maximized. In the numerator, the signal parameter strength λ remains fixed and the likelihood is maximized only for the nuisance parameters, whose values at the maximum are denoted $\hat{\theta}_\lambda$. In the denominator, the likelihood is maximized for both λ and θ . $\hat{\lambda}$ and $\hat{\theta}$ denote the values at which \mathcal{L} reaches its global maximum in the denominator. The lower constraint $0 \leq \hat{\lambda}$ is imposed because the signal strength cannot be negative, while the upper constraint $\hat{\lambda} < \lambda$ guarantees a one-sided confidence interval. The value of the test statistic for the actual observation is denoted q_λ^{obs} . This test statistic [41] differs from that used at LEP and the Tevatron.

To set limits, a modified frequentist CL_s approach is employed [42, 43]. We first define the probabilities to obtain an outcome of an experiment at least as signal-like as the one observed for the background-only and for the signal-plus-background hypotheses. The CL_s quantity is then defined as the ratio of these two probabilities. In the modified frequentist approach, the value of CL_s is required to be less than or equal to α in order to establish a $(1 - \alpha)$ confidence level (CL) exclusion. To quote the upper limit on λ for a given signal at 95% CL, we adjust λ until we reach $\text{CL}_s = 0.05$.

8.1 Exclusion limits in the CMSSM plane

Exclusion limits at 95% CL are determined in the CMSSM ($m_0, m_{1/2}$) plane [44]. The signal cross section is calculated at NLO and next-to-leading-log (NLL) accuracy [26, 45, 46]. At each point in the scan four CL_s values are computed for $\lambda = 1$: the observed, the median expected, and the one standard deviation ($\pm 1\sigma$) expected bands. If the corresponding CL_s value is smaller than 0.05, the point is excluded at 95% CL, resulting in the exclusion limits shown in Fig. 5. The results from both the M_{T2} and $M_{T2}b$ selections are shown in Fig. 5 (top). In Fig. 5 (bottom), the results are combined into a single limit exclusion curve based on the best expected limit at each point of the plane.

The dominant sources of systematic uncertainties on the signal model are found to be the jet energy scale and (for the $M_{T2}b$ analysis) the b-tagging efficiency. These two uncertainties are evaluated at each point of the CMSSM plane, typically ranging from 5 to 25% for the former and from 2 to 6% for the latter. Additionally, a 2.2% uncertainty is associated with the luminosity determination [47]. All these uncertainties are included in the statistical interpretation as nuisance parameters on the signal model.

Observed exclusion limits are also determined when the signal cross section is varied by changing the renormalization and factorization scales by a factor of 2 and using the PDF4LHC recommendation [48] for the PDF uncertainty. The exclusion contours obtained from this method are shown by the dashed curves of Fig. 5 and referred to as theory uncertainties.

The effect of signal contamination in the leptonic control region could be significant, yielding a potential background overprediction of about 1-15%. To account for this effect, the signal yields are corrected by subtracting the expected increase in the background estimate that would occur if the given signal were present in the data.

The results in Fig. 5 (top) establish that the M_{T2} analysis is powerful in the region of large

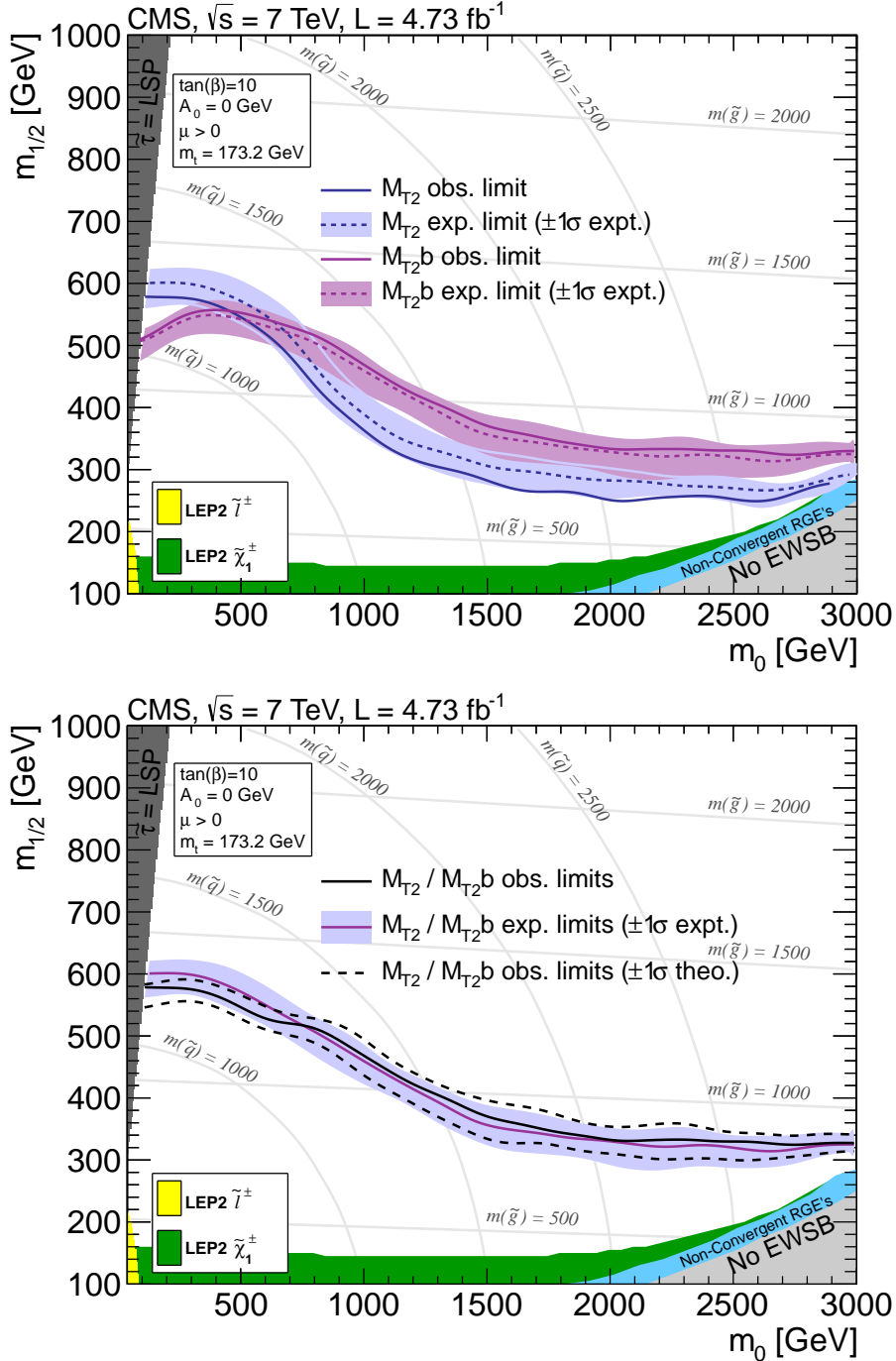


Figure 5: Top: exclusion limit in the CMSSM ($m_0, m_{1/2}$) plane for the M_{T2} and $M_{T2}b$ analyses with $\tan \beta = 10$. Bottom: Combined limit based on the best expected limit at each point.

squark and gluino masses, corresponding to small m_0 and large $m_{1/2}$, while the $M_{T2}b$ analysis increases sensitivity to large squark and small gluino masses, corresponding to large m_0 and small $m_{1/2}$. Conservatively, using the minus one standard deviation (-1σ) theory uncertainty values of the observed limit, we derive absolute lower limits on the squark and gluino masses for the chosen CMSSM parameter set. We find lower limits of $m(\tilde{q}) > 1110$ GeV and $m(\tilde{g}) > 800$ GeV, as well as $m(\tilde{q}) = m(\tilde{g}) > 1180$ GeV assuming equal squark and gluino masses.

8.2 Exclusion limits for simplified model spectra

In this section we interpret the results in terms of simplified model spectra [49], which allow a presentation of the exclusion potential in the context of a larger variety of fundamental models, not necessarily in a supersymmetric framework. We studied the following topologies:

- gluino pair production, with $\tilde{g} \rightarrow q\bar{q}\tilde{\chi}^0$;
- gluino pair production, with $\tilde{g} \rightarrow b\bar{b}\tilde{\chi}^0$;
- gluino pair production, with $\tilde{g} \rightarrow t\bar{t}\tilde{\chi}^0$;
- gluino pair production, with $\tilde{g} \rightarrow q\bar{q}Z\tilde{\chi}^0$.

The last of these models is used to demonstrate the sensitivity of the analysis in a high jet multiplicity topology, since the hadronic decay of the Z boson can lead to (maximally) 8 jets in the final state. In Fig. 6 the 95% CL excluded cross sections are reported as a function of the relevant masses for gluino pair production with $\tilde{g} \rightarrow q\bar{q}\tilde{\chi}^0$ using the M_{T2} analysis, and for $\tilde{g} \rightarrow b\bar{b}\tilde{\chi}^0$, $\tilde{g} \rightarrow t\bar{t}\tilde{\chi}^0$ and $\tilde{g} \rightarrow q\bar{q}Z\tilde{\chi}^0$ using the $M_{T2}b$ analysis. Systematic uncertainties on jet energy scale and on b-tagging efficiencies are taken into account as nuisance parameters on the signal model. To minimize the effect of ISR modeling uncertainties, the region near the diagonal is excluded in the limit setting. Observed, median expected, and one standard deviation ($\pm 1\sigma$ experimental) expected limit curves are derived for the nominal signal cross section. Also shown are the $\pm 1\sigma$ variation in the observed limit when the signal cross section is varied by its theoretical uncertainties.

9 Summary

We have conducted a search for supersymmetry or similar new physics in hadronic final states using the M_{T2} variable calculated from massless pseudojets. M_{T2} is strongly correlated with E_T^{miss} for SUSY processes, yet provides a natural suppression of QCD multijet background. The data set for this analysis corresponds to 4.73 fb^{-1} of integrated luminosity in $\sqrt{s} = 7 \text{ TeV}$ pp collisions collected with the CMS detector during the 2011 LHC run. All candidate events are selected using hadronic triggers. Two complementary analyses are performed. The M_{T2} analysis targets decays of moderately heavy squarks and gluinos, which naturally feature a sizeable E_T^{miss} . This analysis is based on events containing three or more jets and no isolated leptons. We show that the tail of the M_{T2} distribution, obtained after this selection, is sensitive to a potential SUSY signal. A second approach, the $M_{T2}b$ analysis, is designed to increase the sensitivity to events with heavy squarks and light gluinos, in which the E_T^{miss} tends to be smaller. Therefore, the restriction on M_{T2} is relaxed. The effect of the loosened M_{T2} is compensated by requiring at least one b-tagged jet and a larger jet multiplicity, to suppress the QCD multijet background. For both analyses, the standard model backgrounds, arising from QCD multijet, electroweak, and top-quark production processes, are obtained from data control samples and simulation. No excess beyond the standard model expectations is found. Exclusion limits are established in the CMSSM parameter space, as well as for some simplified model spectra. Conservatively, using the minus one standard deviation (-1σ) theory uncertainty values, absolute mass limits in the CMSSM scenario for $\tan\beta = 10$ are found to be $m(\tilde{q}) > 1110 \text{ GeV}$ and $m(\tilde{g}) > 800 \text{ GeV}$, and $m(\tilde{q}) = m(\tilde{g}) > 1180 \text{ GeV}$ assuming equal squark and gluino masses.

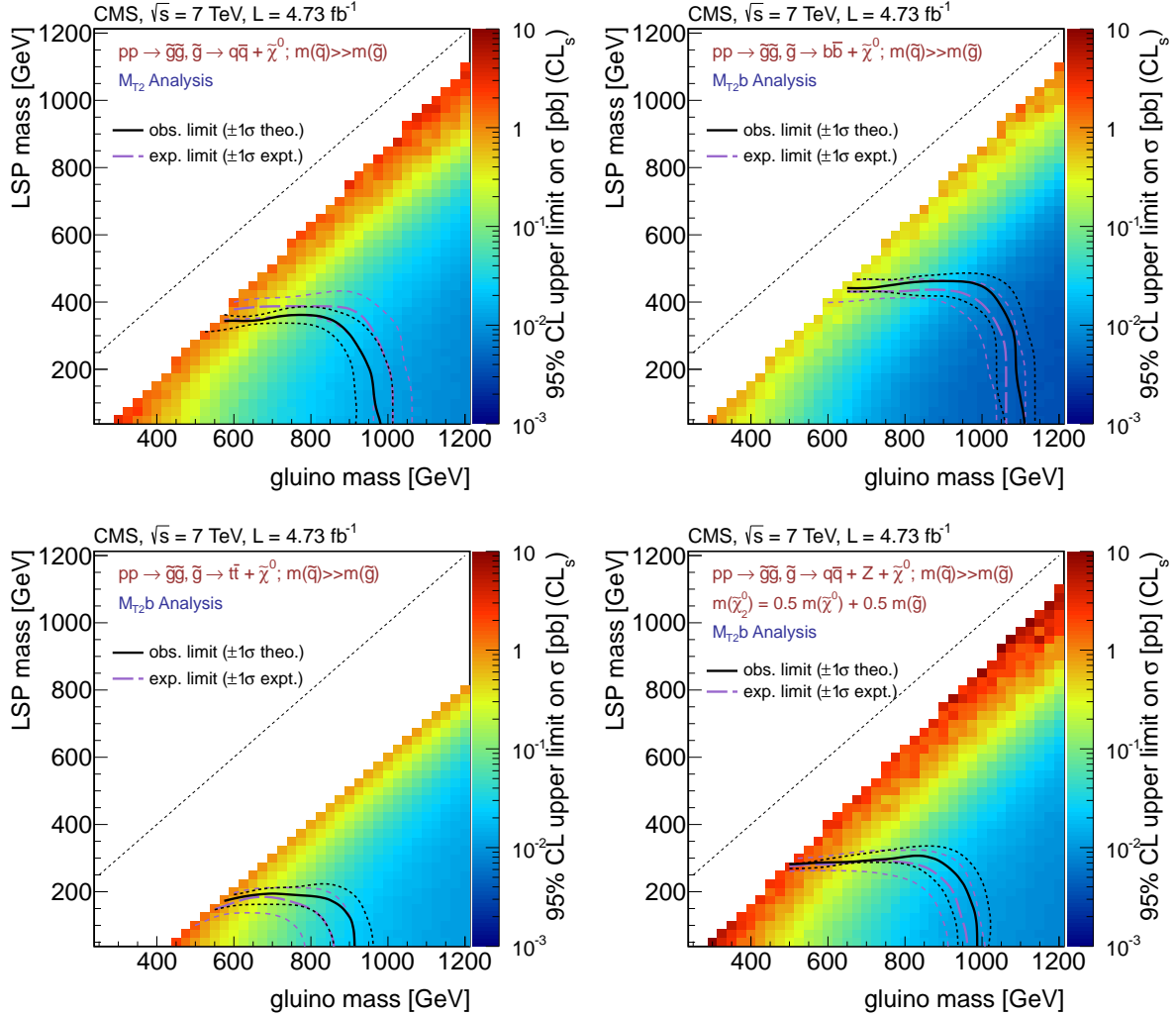


Figure 6: Exclusion limits for simplified model spectra. Upper left: gluino pair production with $\tilde{g} \rightarrow q\bar{q}\tilde{\chi}_1^0$ using the M_{T2} analysis. Upper right: gluino pair production with $\tilde{g} \rightarrow b\bar{b}\tilde{\chi}_1^0$, using the M_{T2b} analysis. Lower left: gluino pair production with $\tilde{g} \rightarrow t\bar{t}\tilde{\chi}_1^0$, using the M_{T2b} analysis. Lower right: gluino pair production with $\tilde{g} \rightarrow q\bar{q}Z\tilde{\chi}_1^0$, using the M_{T2b} analysis. The signal production cross sections are calculated at NLO and NLL accuracy [26, 45, 46].

Acknowledgements

We congratulate our colleagues in the CERN accelerator departments for the excellent performance of the LHC machine. We thank the technical and administrative staff at CERN and other CMS institutes, and acknowledge support from: FMSR (Austria); FNRS and FWO (Belgium); CNPq, CAPES, FAPERJ, and FAPESP (Brazil); MES (Bulgaria); CERN; CAS, MoST, and NSFC (China); COLCIENCIAS (Colombia); MSES (Croatia); RPF (Cyprus); MoER, SF0690030s09 and ERDF (Estonia); Academy of Finland, MEC, and HIP (Finland); CEA and CNRS/IN2P3 (France); BMBF, DFG, and HGF (Germany); GSRT (Greece); OTKA and NKTH (Hungary); DAE and DST (India); IPM (Iran); SFI (Ireland); INFN (Italy); NRF and WCU (Korea); LAS (Lithuania); CINVESTAV, CONACYT, SEP, and UASLP-FAI (Mexico); MSI (New Zealand); PAEC (Pakistan); MSHE and NSC (Poland); FCT (Portugal); JINR (Armenia, Belarus, Georgia, Ukraine, Uzbekistan); MON, RosAtom, RAS and RFBR (Russia); MSTD (Serbia); SEIDI and CPAN (Spain);

Swiss Funding Agencies (Switzerland); NSC (Taipei); TUBITAK and TAEK (Turkey); STFC (United Kingdom); DOE and NSF (USA).

Individuals have received support from the Marie-Curie programme and the European Research Council (European Union); the Leventis Foundation; the A. P. Sloan Foundation; the Alexander von Humboldt Foundation; the Belgian Federal Science Policy Office; the Fonds pour la Formation à la Recherche dans l'Industrie et dans l'Agriculture (FRIA-Belgium); the Agentschap voor Innovatie door Wetenschap en Technologie (IWT-Belgium); the Council of Science and Industrial Research, India; the Iran National Science Foundation (INSF); the Compagnia di San Paolo (Torino); and the HOMING PLUS programme of Foundation for Polish Science, cofinanced from the European Union, Regional Development Fund.

References

- [1] S. P. Martin, “A supersymmetry primer”, (1997). arXiv:hep-ph/9709356.
- [2] C. G. Lester and D. J. Summers, “Measuring masses of semi-invisibly decaying particles pair produced at hadron colliders”, *Phys. Lett. B* **463** (1999) 99, doi:10.1016/S0370-2693(99)00945-4, arXiv:hep-ph/9906349.
- [3] A. Barr, C. Lester, and P. Stephens, “ M_{T2} : The truth behind the glamour”, *J. Phys. G* **29** (2003) 2343, doi:10.1088/0954-3899/29/10/304, arXiv:hep-ph/0304226.
- [4] CMS Collaboration, “Search for new physics with jets and missing transverse momentum in pp collisions at $\sqrt{s} = 7 \text{ TeV}$ ”, *J. High Energy Phys.* **08** (2011) 155, doi:10.1007/JHEP08(2011)155, arXiv:1106.4503.
- [5] CMS Collaboration, “Inclusive search for squarks and gluinos in pp collisions at $\sqrt{s} = 7 \text{ TeV}$ ”, *Phys. Rev. D* **85** (2012) 012004, doi:10.1103/PhysRevD.85.012004, arXiv:1107.1279.
- [6] CMS Collaboration, “Search for supersymmetry in pp collisions at 7 TeV in events with jets and missing transverse energy”, *Phys. Lett. B* **698** (2011) 196, doi:10.1016/j.physletb.2011.03.021, arXiv:1101.1628.
- [7] CMS Collaboration, “Search for supersymmetry at the LHC in events with jets and missing transverse energy”, *Phys. Rev. Lett.* **107** (2011) 221804, doi:10.1103/PhysRevLett.107.221804, arXiv:1109.2352.
- [8] ATLAS Collaboration, “Search for squarks and gluinos using final states with jets and missing transverse momentum with the ATLAS detector in proton-proton collisions”, *Phys. Lett. B* **710** (2012) 67, doi:10.1016/j.physletb.2012.02.051, arXiv:1109.6572.
- [9] ATLAS Collaboration, “Search for squarks and gluinos using final states with jets and missing transverse momentum with the ATLAS detector in $\sqrt{s} = 7 \text{ TeV}$ proton-proton collisions”, *Phys. Lett. B* **701** (2011) 186, doi:10.1016/j.physletb.2011.05.061, arXiv:1102.5290.
- [10] ATLAS Collaboration, “Search for new phenomena in final states with large jet multiplicities and missing transverse momentum using $\sqrt{s} = 7 \text{ TeV}$ pp collisions with the ATLAS detector”, *J. High Energy Phys.* **11** (2011) 099, doi:10.1007/JHEP11(2011)099, arXiv:1110.2299.

- [11] ATLAS Collaboration, “Hunt for new phenomena using large jet multiplicities and missing transverse momentum with ATLAS in 4.7 fb^{-1} of $\sqrt{s} = 7 \text{ TeV}$ proton-proton collisions”, (2012). arXiv:1206.1760. Submitted to *J. High Energy Phys.*
- [12] UA1 Collaboration, “Experimental observation of isolated large transverse energy electrons with associated missing energy at $\sqrt{s} = 540 \text{ GeV}$ ”, *Phys. Lett. B* **122** (1983) 103, doi:10.1016/0370-2693(83)91177-2.
- [13] W. S. Cho, K. Choi, Y. G. Kim et al., “Measuring superparticle masses at hadron collider using the transverse mass kink”, *J. High Energy Phys.* **02** (2008) 035, doi:10.1088/1126-6708/2008/02/035, arXiv:0711.4526.
- [14] M. Burns, K. Kong, K. T. Matchev et al., “Using subsystem M_{T2} for complete mass determinations in decay chains with missing energy at hadron colliders”, *J. High Energy Phys.* **03** (2009) 143, doi:10.1088/1126-6708/2009/03/143, arXiv:0810.5576.
- [15] H.-C. Cheng and Z. Han, “Minimal kinematic constraints and M_{T2} ”, *J. High Energy Phys.* **12** (2008) 063, doi:10.1088/1126-6708/2008/12/063, arXiv:0810.5178.
- [16] A. J. Barr and C. Gwenlan, “The race for supersymmetry: using M_{T2} for discovery”, *Phys. Rev. D* **80** (2009) 074007, doi:10.1103/PhysRevD.80.074007, arXiv:0907.2713.
- [17] CMS Collaboration, “CMS technical design report, volume II: Physics performance”, *J. Phys. G* **34** (2007) 995, doi:10.1088/0954-3899/34/6/S01.
- [18] T. Sjöstrand, S. Mrenna, and P. Z. Skands, “PYTHIA 6.4 physics and manual”, *J. High Energy Phys.* **05** (2006) 026, doi:10.1088/1126-6708/2006/05/026, arXiv:hep-ph/0603175.
- [19] CMS Collaboration, “The CMS experiment at the CERN LHC”, *JINST* **03** (2008) S08004, doi:10.1088/1748-0221/3/08/S08004.
- [20] J. Alwall, M. Herquet, F. Maltoni et al., “MadGraph 5 : Going beyond”, *J. High Energy Phys.* **06** (2011) 128, doi:10.1007/JHEP06(2011)128, arXiv:1106.0522.
- [21] GEANT4 Collaboration, “GEANT4: A simulation toolkit”, *Nucl. Instrum. Methods Phys. Res. A* **506** (2003) 250, doi:10.1016/S0168-9002(03)01368-8.
- [22] B. C. Allanach, “SOFTSUSY: A program for calculating supersymmetric spectra”, *Comput. Phys. Commun.* **143** (2002) 305, doi:10.1016/S0010-4655(01)00460-X.
- [23] M. Muhlleitner, A. Djouadi, and Y. Mambrini, “SDECAY: A fortran code for the decays of the supersymmetric particles in the MSSM”, *Comput. Phys. Commun.* **168** (2005) 46, doi:10.1016/j.cpc.2005.01.012, arXiv:hep-ph/0311167.
- [24] G. L. Kane, C. Kolda, L. Roszkowski et al., “Study of constrained minimal supersymmetry”, *Phys. Rev. D* **49** (1994) 6173, doi:10.1103/PhysRevD.49.6173, arXiv:hep-ph/9312272.
- [25] J. Pumplin, D. R. Stump, J. Huston et al., “New generation of parton distributions with uncertainties from global QCD analysis”, *J. High Energy Phys.* **07** (2002) 012, doi:10.1088/1126-6708/2002/07/012, arXiv:hep-ph/0201195.
- [26] W. Beenakker, R. Hopker, and M. Spira, “PROSPINO: A program for the PROduction of Supersymmetric Particles In Next-to-leading Order QCD”, (1996). arXiv:hep-ph/9611232.

- [27] CMS Collaboration, “Particle flow event reconstruction in CMS and performance for jets, taus and MET”, CMS Physics Analysis Summary CMS-PAS-PFT-09-001, (2009).
- [28] CMS Collaboration, “Electron reconstruction and identification at $\sqrt{s} = 7 \text{ TeV}$ ”, CMS Physics Analysis Summary CMS-PAS-EGM-10-004, (2010).
- [29] CMS Collaboration, “Particle-flow commissioning with muons and electrons from J/Psi and W events at 7 TeV”, CMS Physics Analysis Summary CMS-PAS-PFT-10-003, (2010).
- [30] CMS Collaboration, “Performance of CMS muon reconstruction in pp collision events at $\sqrt{s} = 7 \text{ TeV}$ ”, CMS Physics Analysis Summary CMS-PAS-MUO-10-002, (2011).
- [31] M. Cacciari, G. P. Salam, and G. Soyez, “The anti- k_t jet clustering algorithm”, *J. High Energy Phys.* **04** (2008) 063, doi:10.1088/1126-6708/2008/04/063, arXiv:0802.1189.
- [32] CMS Collaboration, “Jet performance in pp collisions at $\sqrt{s} = 7 \text{ TeV}$ ”, CMS Physics Analysis Summary CMS-PAS-JME-10-003, (2010).
- [33] CMS Collaboration, “Commissioning of the particle-flow reconstruction in minimum-bias and jet events from pp collisions at 7 TeV”, CMS Physics Analysis Summary CMS-PAS-PFT-10-002, (2010).
- [34] CMS Collaboration, “Determination of jet energy calibration and transverse momentum resolution in CMS”, *JINST* **06** (2011) P11002, doi:10.1088/1748-0221/6/11/P11002, arXiv:1107.4277.
- [35] M. Cacciari and G. P. Salam, “Pileup subtraction using jet areas”, *Phys. Lett. B* **659** (2008) 119, doi:10.1016/j.physletb.2007.09.077, arXiv:0707.1378.
- [36] M. Cacciari, G. P. Salam, and G. Soyez, “The catchment area of jets”, *J. High Energy Phys.* **04** (2008) 005, doi:10.1088/1126-6708/2008/04/005, arXiv:0802.1188.
- [37] CMS Collaboration, “Commissioning of b-jet identification with pp collisions at $\sqrt{s} = 7 \text{ TeV}$ ”, CMS Physics Analysis Summary CMS-PAS-BTV-10-001, (2010).
- [38] CMS Collaboration, “Tracking and primary vertex results in first 7 TeV collisions”, CMS Physics Analysis Summary CMS-PAS-TRK-10-005, (2010).
- [39] CMS Collaboration, “Tau identification in CMS”, CMS Physics Analysis Summary CMS-PAS-PFT-11-001, (2011).
- [40] CMS Collaboration, “Isolated photon reconstruction and identification at $\sqrt{s} = 7 \text{ TeV}$ ”, CMS Physics Analysis Summary CMS-PAS-EGM-10-006, (2011).
- [41] ATLAS and CMS Collaborations, “Procedure for the LHC Higgs boson search combination in summer 2011”, ATL-PHYS-PUB-2011-11, CMS NOTE-2011/005, (2011).
- [42] T. Junk, “Confidence level computation for combining searches with small statistics”, *Nucl. Instrum. Methods Phys. Res. A* **434** (1999) 435, doi:10.1016/S0168-9002(99)00498-2, arXiv:hep-ex/9902006.
- [43] A. L. Read, “Presentation of search results: The CL_s technique”, *J. Phys. G* **28** (2002) 2693, doi:10.1088/0954-3899/28/10/313.

- [44] K. Matchev and R. Remington, "Updated templates for the interpretation of LHC results on supersymmetry in the context of mSUGRA", (2012). arXiv:1202.6580.
- [45] A. Kulesza and L. Motyka, "Threshold resummation for squark-antisquark and gluino-pair production at the LHC", *Phys. Rev. Lett.* **102** (2009) 111802,
doi:10.1103/PhysRevLett.102.111802, arXiv:0807.2405.
- [46] M. Krämer, A. Kulesza, R. van der Leeuw et al., "Supersymmetry production cross sections in pp collisions at $\sqrt{s} = 7 \text{ TeV}$ ", (2012). arXiv:1206.2892.
- [47] CMS Collaboration, "Absolute calibration of the luminosity measurement at CMS: Winter 2012 update", CMS Physics Analysis Summary CMS-PAS-SMP-12-008, (2012).
- [48] M. Botje, J. Butterworth, A. Cooper-Sarkar et al., "The PDF4LHC working group interim recommendations", (2011). arXiv:1101.0538.
- [49] LHC New Physics Working Group Collaboration, "Simplified models for LHC new physics searches", (2011). arXiv:1105.2838.

A The CMS Collaboration

Yerevan Physics Institute, Yerevan, Armenia

S. Chatrchyan, V. Khachatryan, A.M. Sirunyan, A. Tumasyan

Institut für Hochenergiephysik der OeAW, Wien, Austria

W. Adam, T. Bergauer, M. Dragicevic, J. Erö, C. Fabjan¹, M. Friedl, R. Frühwirth¹, V.M. Ghete, J. Hammer, N. Hörmann, J. Hrubec, M. Jeitler¹, W. Kiesenhofer, V. Knünz, M. Krammer¹, D. Liko, I. Mikulec, M. Pernicka[†], B. Rahbaran, C. Rohringer, H. Rohringer, R. Schöfbeck, J. Strauss, A. Taurok, P. Wagner, W. Waltenberger, G. Walzel, E. Widl, C.-E. Wulz¹

National Centre for Particle and High Energy Physics, Minsk, Belarus

V. Mossolov, N. Shumeiko, J. Suarez Gonzalez

Universiteit Antwerpen, Antwerpen, Belgium

S. Bansal, T. Cornelis, E.A. De Wolf, X. Janssen, S. Luyckx, L. Mucibello, S. Ochesanu, B. Roland, R. Rougny, M. Selvaggi, Z. Staykova, H. Van Haevermaet, P. Van Mechelen, N. Van Remortel, A. Van Spilbeeck

Vrije Universiteit Brussel, Brussel, Belgium

F. Blekman, S. Blyweert, J. D'Hondt, R. Gonzalez Suarez, A. Kalogeropoulos, M. Maes, A. Olbrechts, W. Van Doninck, P. Van Mulders, G.P. Van Onsem, I. Villella

Université Libre de Bruxelles, Bruxelles, Belgium

B. Clerbaux, G. De Lentdecker, V. Dero, A.P.R. Gay, T. Hreus, A. Léonard, P.E. Marage, T. Reis, L. Thomas, C. Vander Velde, P. Vanlaer, J. Wang

Ghent University, Ghent, Belgium

V. Adler, K. Beernaert, A. Cimmino, S. Costantini, G. Garcia, M. Grunewald, B. Klein, J. Lellouch, A. Marinov, J. Mccartin, A.A. Ocampo Rios, D. Ryckbosch, N. Strobbe, F. Thyssen, M. Tytgat, P. Verwilligen, S. Walsh, E. Yazgan, N. Zaganidis

Université Catholique de Louvain, Louvain-la-Neuve, Belgium

S. Basegmez, G. Bruno, R. Castello, A. Caudron, L. Ceard, C. Delaere, T. du Pree, D. Favart, L. Forthomme, A. Giannanco², J. Hollar, V. Lemaitre, J. Liao, O. Militaru, C. Nuttens, D. Pagano, L. Perrini, A. Pin, K. Piotrkowski, N. Schul, J.M. Vizan Garcia

Université de Mons, Mons, Belgium

N. Beliy, T. Caebergs, E. Daubie, G.H. Hammad

Centro Brasileiro de Pesquisas Fisicas, Rio de Janeiro, Brazil

G.A. Alves, M. Correa Martins Junior, D. De Jesus Damiao, T. Martins, M.E. Pol, M.H.G. Souza

Universidade do Estado do Rio de Janeiro, Rio de Janeiro, Brazil

W.L. Aldá Júnior, W. Carvalho, A. Custódio, E.M. Da Costa, C. De Oliveira Martins, S. Fonseca De Souza, D. Matos Figueiredo, L. Mundim, H. Nogima, V. Oguri, W.L. Prado Da Silva, A. Santoro, L. Soares Jorge, A. Sznajder

Instituto de Física Teórica, Universidade Estadual Paulista, São Paulo, Brazil

C.A. Bernardes³, F.A. Dias⁴, T.R. Fernandez Perez Tomei, E. M. Gregores³, C. Lagana, F. Marinho, P.G. Mercadante³, S.F. Novaes, Sandra S. Padula

Institute for Nuclear Research and Nuclear Energy, Sofia, Bulgaria

V. Genchev⁵, P. Iaydjiev⁵, S. Piperov, M. Rodozov, S. Stoykova, G. Sultanov, V. Tcholakov, R. Trayanov, M. Vutova

University of Sofia, Sofia, Bulgaria

A. Dimitrov, R. Hadjiiska, V. Kozuharov, L. Litov, B. Pavlov, P. Petkov

Institute of High Energy Physics, Beijing, China

J.G. Bian, G.M. Chen, H.S. Chen, C.H. Jiang, D. Liang, S. Liang, X. Meng, J. Tao, J. Wang, X. Wang, Z. Wang, H. Xiao, M. Xu, J. Zang, Z. Zhang

State Key Lab. of Nucl. Phys. and Tech., Peking University, Beijing, China

C. Asawatangtrakuldee, Y. Ban, S. Guo, Y. Guo, W. Li, S. Liu, Y. Mao, S.J. Qian, H. Teng, S. Wang, B. Zhu, W. Zou

Universidad de Los Andes, Bogota, Colombia

C. Avila, J.P. Gomez, B. Gomez Moreno, A.F. Osorio Oliveros, J.C. Sanabria

Technical University of Split, Split, CroatiaN. Godinovic, D. Lelas, R. Plestina⁶, D. Polic, I. Puljak⁵**University of Split, Split, Croatia**

Z. Antunovic, M. Kovac

Institute Rudjer Boskovic, Zagreb, Croatia

V. Brigljevic, S. Duric, K. Kadija, J. Luetic, S. Morovic

University of Cyprus, Nicosia, Cyprus

A. Attikis, M. Galanti, G. Mavromanolakis, J. Mousa, C. Nicolaou, F. Ptochos, P.A. Razis

Charles University, Prague, Czech Republic

M. Finger, M. Finger Jr.

Academy of Scientific Research and Technology of the Arab Republic of Egypt, Egyptian Network of High Energy Physics, Cairo, EgyptY. Assran⁷, S. Elgammal⁸, A. Ellithi Kamel⁹, S. Khalil⁸, M.A. Mahmoud¹⁰, A. Radi^{11,12}**National Institute of Chemical Physics and Biophysics, Tallinn, Estonia**

M. Kadastik, M. Müntel, M. Raidal, L. Rebane, A. Tiko

Department of Physics, University of Helsinki, Helsinki, Finland

V. Azzolini, P. Eerola, G. Fedi, M. Voutilainen

Helsinki Institute of Physics, Helsinki, Finland

J. Hätkönen, A. Heikkinen, V. Karimäki, R. Kinnunen, M.J. Kortelainen, T. Lampén, K. Lassila-Perini, S. Lehti, T. Lindén, P. Luukka, T. Mäenpää, T. Peltola, E. Tuominen, J. Tuominiemi, E. Tuovinen, D. Ungaro, L. Wendland

Lappeenranta University of Technology, Lappeenranta, Finland

K. Banzuzi, A. Karjalainen, A. Korppela, T. Tuuva

DSM/IRFU, CEA/Saclay, Gif-sur-Yvette, France

M. Besancon, S. Choudhury, M. Dejardin, D. Denegri, B. Fabbro, J.L. Faure, F. Ferri, S. Ganjour, A. Givernaud, P. Gras, G. Hamel de Monchenault, P. Jarry, E. Locci, J. Malcles, L. Millischer, A. Nayak, J. Rander, A. Rosowsky, I. Shreyber, M. Titov

Laboratoire Leprince-Ringuet, Ecole Polytechnique, IN2P3-CNRS, Palaiseau, FranceS. Baffioni, F. Beaudette, L. Benhabib, L. Bianchini, M. Bluj¹³, C. Broutin, P. Busson, C. Charlot, N. Daci, T. Dahms, L. Dobrzynski, R. Granier de Cassagnac, M. Haguenauer, P. Miné, C. Mironov, M. Nguyen, C. Ochando, P. Paganini, D. Sabes, R. Salerno, Y. Sirois, C. Veelken, A. Zabi

Institut Pluridisciplinaire Hubert Curien, Université de Strasbourg, Université de Haute Alsace Mulhouse, CNRS/IN2P3, Strasbourg, France

J.-L. Agram¹⁴, J. Andrea, D. Bloch, D. Bodin, J.-M. Brom, M. Cardaci, E.C. Chabert, C. Collard, E. Conte¹⁴, F. Drouhin¹⁴, C. Ferro, J.-C. Fontaine¹⁴, D. Gelé, U. Goerlach, P. Juillot, A.-C. Le Bihan, P. Van Hove

Centre de Calcul de l’Institut National de Physique Nucléaire et de Physique des Particules (IN2P3), Villeurbanne, France

F. Fassi, D. Mercier

Université de Lyon, Université Claude Bernard Lyon 1, CNRS-IN2P3, Institut de Physique Nucléaire de Lyon, Villeurbanne, France

S. Beauceron, N. Beaupere, O. Bondu, G. Boudoul, J. Chasserat, R. Chierici⁵, D. Contardo, P. Depasse, H. El Mamouni, J. Fay, S. Gascon, M. Gouzevitch, B. Ille, T. Kurca, M. Lethuillier, L. Mirabito, S. Perries, V. Sordini, S. Tosi, Y. Tschudi, P. Verdier, S. Viret

E. Andronikashvili Institute of Physics, Academy of Science, Tbilisi, Georgia

L. Rurua

RWTH Aachen University, I. Physikalisches Institut, Aachen, Germany

G. Anagnostou, S. Beranek, M. Edelhoff, L. Feld, N. Heracleous, O. Hindrichs, R. Jussen, K. Klein, J. Merz, A. Ostapchuk, A. Perieanu, F. Raupach, J. Sammet, S. Schael, D. Sprenger, H. Weber, B. Wittmer, V. Zhukov¹⁵

RWTH Aachen University, III. Physikalisches Institut A, Aachen, Germany

M. Ata, J. Caudron, E. Dietz-Laursonn, D. Duchardt, M. Erdmann, R. Fischer, A. Güth, T. Hebbeker, C. Heidemann, K. Hoepfner, D. Klingebiel, P. Kreuzer, J. Lingemann, C. Magass, M. Merschmeyer, A. Meyer, M. Olschewski, P. Papacz, H. Pieta, H. Reithler, S.A. Schmitz, L. Sonnenschein, J. Steggemann, D. Teyssier, M. Weber

RWTH Aachen University, III. Physikalisches Institut B, Aachen, Germany

M. Bontenackels, V. Cherepanov, G. Flügge, H. Geenen, M. Geisler, W. Haj Ahmad, F. Hoehle, B. Kargoll, T. Kress, Y. Kuessel, A. Nowack, L. Perchalla, O. Pooth, J. Rennefeld, P. Sauerland, A. Stahl

Deutsches Elektronen-Synchrotron, Hamburg, Germany

M. Aldaya Martin, J. Behr, W. Behrenhoff, U. Behrens, M. Bergholz¹⁶, A. Bethani, K. Borras, A. Burgmeier, A. Cakir, L. Calligaris, A. Campbell, E. Castro, F. Costanza, D. Dammann, C. Diez Pardos, G. Eckerlin, D. Eckstein, G. Flucke, A. Geiser, I. Glushkov, P. Gunnellini, S. Habib, J. Hauk, G. Hellwig, H. Jung, M. Kasemann, P. Katsas, C. Kleinwort, H. Kluge, A. Knutsson, M. Krämer, D. Krücker, E. Kuznetsova, W. Lange, W. Lohmann¹⁶, B. Lutz, R. Mankel, I. Marfin, M. Marienfeld, I.-A. Melzer-Pellmann, A.B. Meyer, J. Mnich, A. Mussgiller, S. Naumann-Emme, J. Olzem, H. Perrey, A. Petrukhin, D. Pitzl, A. Raspereza, P.M. Ribeiro Cipriano, C. Riedl, E. Ron, M. Rosin, J. Salfeld-Nebgen, R. Schmidt¹⁶, T. Schoerner-Sadenius, N. Sen, A. Spiridonov, M. Stein, R. Walsh, C. Wissing

University of Hamburg, Hamburg, Germany

C. Autermann, V. Blobel, J. Draeger, H. Enderle, J. Erfle, U. Gebbert, M. Görner, T. Hermanns, R.S. Höing, K. Kaschube, G. Kaussen, H. Kirschenmann, R. Klanner, J. Lange, B. Mura, F. Nowak, T. Peiffer, N. Pietsch, D. Rathjens, C. Sander, H. Schettler, P. Schleper, E. Schlieckau, A. Schmidt, M. Schröder, T. Schum, M. Seidel, V. Sola, H. Stadie, G. Steinbrück, J. Thomsen, L. Vanelderen

Institut für Experimentelle Kernphysik, Karlsruhe, Germany

C. Barth, J. Berger, C. Böser, T. Chwalek, W. De Boer, A. Descroix, A. Dierlamm, M. Feindt, M. Guthoff⁵, C. Hackstein, F. Hartmann, T. Hauth⁵, M. Heinrich, H. Held, K.H. Hoffmann, S. Honc, I. Katkov¹⁵, J.R. Komaragiri, P. Lobelle Pardo, D. Martschei, S. Mueller, Th. Müller, M. Niegel, A. Nürnberg, O. Oberst, A. Oehler, J. Ott, G. Quast, K. Rabbertz, F. Ratnikov, N. Ratnikova, S. Röcker, A. Scheurer, F.-P. Schilling, G. Schott, H.J. Simonis, F.M. Stober, D. Troendle, R. Ulrich, J. Wagner-Kuhr, S. Wayand, T. Weiler, M. Zeise

Institute of Nuclear Physics "Demokritos", Aghia Paraskevi, Greece

G. Daskalakis, T. Geralis, S. Kesisoglou, A. Kyriakis, D. Loukas, I. Manolakos, A. Markou, C. Markou, C. Mavrommatis, E. Ntomari

University of Athens, Athens, Greece

L. Gouskos, T.J. Mertzimekis, A. Panagiotou, N. Saoulidou

University of Ioánnina, Ioánnina, Greece

I. Evangelou, C. Foudas⁵, P. Kokkas, N. Manthos, I. Papadopoulos, V. Patras

KFKI Research Institute for Particle and Nuclear Physics, Budapest, Hungary

G. Bencze, C. Hajdu⁵, P. Hidas, D. Horvath¹⁷, F. Sikler, V. Vesztergombi¹⁸

Institute of Nuclear Research ATOMKI, Debrecen, Hungary

N. Beni, S. Czellar, J. Molnar, J. Palinkas, Z. Szillasi

University of Debrecen, Debrecen, Hungary

J. Karancsi, P. Raics, Z.L. Trocsanyi, B. Ujvari

Panjab University, Chandigarh, India

S.B. Beri, V. Bhatnagar, N. Dhingra, R. Gupta, M. Jindal, M. Kaur, M.Z. Mehta, N. Nishu, L.K. Saini, A. Sharma, J. Singh

University of Delhi, Delhi, India

Ashok Kumar, Arun Kumar, S. Ahuja, A. Bhardwaj, B.C. Choudhary, S. Malhotra, M. Naimuddin, K. Ranjan, V. Sharma, R.K. Shrivpuri

Saha Institute of Nuclear Physics, Kolkata, India

S. Banerjee, S. Bhattacharya, S. Dutta, B. Gomber, Sa. Jain, Sh. Jain, R. Khurana, S. Sarkar, M. Sharan

Bhabha Atomic Research Centre, Mumbai, India

A. Abdulsalam, R.K. Choudhury, D. Dutta, S. Kailas, V. Kumar, P. Mehta, A.K. Mohanty⁵, L.M. Pant, P. Shukla

Tata Institute of Fundamental Research - EHEP, Mumbai, India

T. Aziz, S. Ganguly, M. Guchait¹⁹, M. Maity²⁰, G. Majumder, K. Mazumdar, G.B. Mohanty, B. Parida, K. Sudhakar, N. Wickramage

Tata Institute of Fundamental Research - HEGR, Mumbai, India

S. Banerjee, S. Dugad

Institute for Research in Fundamental Sciences (IPM), Tehran, Iran

H. Arfaei, H. Bakhshiansohi²¹, S.M. Etesami²², A. Fahim²¹, M. Hashemi, H. Hesari, A. Jafari²¹, M. Khakzad, M. Mohammadi Najafabadi, S. Paktnat Mehdiabadi, B. Safarzadeh²³, M. Zeinali²²

INFN Sezione di Bari ^a, Università di Bari ^b, Politecnico di Bari ^c, Bari, Italy

M. Abbrescia^{a,b}, L. Barbone^{a,b}, C. Calabria^{a,b,5}, S.S. Chhibra^{a,b}, A. Colaleo^a, D. Creanza^{a,c},

N. De Filippis^{a,c,5}, M. De Palma^{a,b}, L. Fiore^a, G. Iaselli^{a,c}, L. Lusito^{a,b}, G. Maggi^{a,c}, M. Maggi^a, B. Marangelli^{a,b}, S. My^{a,c}, S. Nuzzo^{a,b}, N. Pacifico^{a,b}, A. Pompili^{a,b}, G. Pugliese^{a,c}, G. Selvaggi^{a,b}, L. Silvestris^a, G. Singh^{a,b}, R. Venditti, G. Zito^a

INFN Sezione di Bologna ^a, Università di Bologna ^b, Bologna, Italy

G. Abbiendi^a, A.C. Benvenuti^a, D. Bonacorsi^{a,b}, S. Braibant-Giacomelli^{a,b}, L. Brigliadori^{a,b}, P. Capiluppi^{a,b}, A. Castro^{a,b}, F.R. Cavallo^a, M. Cuffiani^{a,b}, G.M. Dallavalle^a, F. Fabbri^a, A. Fanfani^{a,b}, D. Fasanella^{a,b,5}, P. Giacomelli^a, C. Grandi^a, L. Guiducci^{a,b}, S. Marcellini^a, G. Masetti^a, M. Meneghelli^{a,b,5}, A. Montanari^a, F.L. Navarria^{a,b}, F. Odorici^a, A. Perrotta^a, F. Primavera^{a,b}, A.M. Rossi^{a,b}, T. Rovelli^{a,b}, G. Siroli^{a,b}, R. Travaglini^{a,b}

INFN Sezione di Catania ^a, Università di Catania ^b, Catania, Italy

S. Albergo^{a,b}, G. Cappello^{a,b}, M. Chiorboli^{a,b}, S. Costa^{a,b}, R. Potenza^{a,b}, A. Tricomi^{a,b}, C. Tuve^{a,b}

INFN Sezione di Firenze ^a, Università di Firenze ^b, Firenze, Italy

G. Barbagli^a, V. Ciulli^{a,b}, C. Civinini^a, R. D'Alessandro^{a,b}, E. Focardi^{a,b}, S. Frosali^{a,b}, E. Gallo^a, S. Gonzi^{a,b}, M. Meschini^a, S. Paoletti^a, G. Sguazzoni^a, A. Tropiano^{a,5}

INFN Laboratori Nazionali di Frascati, Frascati, Italy

L. Benussi, S. Bianco, S. Colafranceschi²⁴, F. Fabbri, D. Piccolo

INFN Sezione di Genova, Genova, Italy

P. Fabbricatore, R. Musenich

INFN Sezione di Milano-Bicocca ^a, Università di Milano-Bicocca ^b, Milano, Italy

A. Benaglia^{a,b,5}, F. De Guio^{a,b}, L. Di Matteo^{a,b,5}, S. Fiorendi^{a,b}, S. Gennai^{a,5}, A. Ghezzi^{a,b}, S. Malvezzi^a, R.A. Manzoni^{a,b}, A. Martelli^{a,b}, A. Massironi^{a,b,5}, D. Menasce^a, L. Moroni^a, M. Paganoni^{a,b}, D. Pedrini^a, S. Ragazzi^{a,b}, N. Redaelli^a, S. Sala^a, T. Tabarelli de Fatis^{a,b}

INFN Sezione di Napoli ^a, Università di Napoli "Federico II" ^b, Napoli, Italy

S. Buontempo^a, C.A. Carrillo Montoya^{a,5}, N. Cavallo^{a,25}, A. De Cosa^{a,b,5}, O. Dogangun^{a,b}, F. Fabozzi^{a,25}, A.O.M. Iorio^a, L. Lista^a, S. Meola^{a,26}, M. Merola^{a,b}, P. Paolucci^{a,5}

INFN Sezione di Padova ^a, Università di Padova ^b, Università di Trento (Trento) ^c, Padova, Italy

P. Azzi^a, N. Bacchetta^{a,5}, P. Bellan^{a,b}, D. Bisello^{a,b}, A. Branca^{a,5}, R. Carlin^{a,b}, P. Checchia^a, T. Dorigo^a, U. Dosselli^a, F. Gasparini^{a,b}, U. Gasparini^{a,b}, A. Gozzelino^a, K. Kanishchev^{a,c}, S. Lacaprara^a, I. Lazzizzera^{a,c}, M. Margoni^{a,b}, A.T. Meneguzzo^{a,b}, M. Nespolo^{a,5}, J. Pazzini^a, P. Ronchese^{a,b}, F. Simonetto^{a,b}, E. Torassa^a, S. Vanini^{a,b}, P. Zotto^{a,b}, A. Zucchetta^a, G. Zumerle^{a,b}

INFN Sezione di Pavia ^a, Università di Pavia ^b, Pavia, Italy

M. Gabusi^{a,b}, S.P. Ratti^{a,b}, C. Riccardi^{a,b}, P. Torre^{a,b}, P. Vitulo^{a,b}

INFN Sezione di Perugia ^a, Università di Perugia ^b, Perugia, Italy

M. Biasini^{a,b}, G.M. Bilei^a, L. Fanò^{a,b}, P. Lariccia^{a,b}, A. Lucaroni^{a,b,5}, G. Mantovani^{a,b}, M. Menichelli^a, A. Nappi^{a,b}, F. Romeo^{a,b}, A. Saha^a, A. Santocchia^{a,b}, S. Taroni^{a,b,5}

INFN Sezione di Pisa ^a, Università di Pisa ^b, Scuola Normale Superiore di Pisa ^c, Pisa, Italy

P. Azzurri^{a,c}, G. Bagliesi^a, T. Boccali^a, G. Broccolo^{a,c}, R. Castaldi^a, R.T. D'Agnolo^{a,c}, R. Dell'Orso^a, F. Fiori^{a,b,5}, L. Foà^{a,c}, A. Giassi^a, A. Kraan^a, F. Ligabue^{a,c}, T. Lomtadze^a, L. Martinia²⁷, A. Messineo^{a,b}, F. Palla^a, A. Rizzi^{a,b}, A.T. Serban^{a,28}, P. Spagnolo^a, P. Squillaciotti^{a,5}, R. Tenchini^a, G. Tonelli^{a,b,5}, A. Venturi^{a,5}, P.G. Verdini^a

INFN Sezione di Roma ^a, Università di Roma "La Sapienza" ^b, Roma, Italy

L. Barone^{a,b}, F. Cavallari^a, D. Del Re^{a,b,5}, M. Diemoz^a, M. Grassi^{a,b,5}, E. Longo^{a,b}

P. Meridiani^{a,5}, F. Micheli^{a,b}, S. Nourbakhsh^{a,b}, G. Organtini^{a,b}, R. Paramatti^a, S. Rahatlou^{a,b}, M. Sigamani^a, L. Soffi^{a,b}

INFN Sezione di Torino ^a, Università di Torino ^b, Università del Piemonte Orientale (Novara) ^c, Torino, Italy

N. Amapane^{a,b}, R. Arcidiacono^{a,c}, S. Argiro^{a,b}, M. Arneodo^{a,c}, C. Biino^a, N. Cartiglia^a, M. Costa^{a,b}, N. Demaria^a, A. Graziano^{a,b}, C. Mariotti^{a,5}, S. Maselli^a, E. Migliore^{a,b}, V. Monaco^{a,b}, M. Musich^{a,5}, M.M. Obertino^{a,c}, N. Pastrone^a, M. Pelliccioni^a, A. Potenza^{a,b}, A. Romero^{a,b}, M. Ruspa^{a,c}, R. Sacchi^{a,b}, A. Solano^{a,b}, A. Staiano^a, A. Vilela Pereira^a

INFN Sezione di Trieste ^a, Università di Trieste ^b, Trieste, Italy

S. Belforte^a, V. Candelise^{a,b}, F. Cossutti^a, G. Della Ricca^{a,b}, B. Gobbo^a, M. Marone^{a,b,5}, D. Montanino^{a,b,5}, A. Penzo^a, A. Schizzi^{a,b}

Kangwon National University, Chunchon, Korea

S.G. Heo, T.Y. Kim, S.K. Nam

Kyungpook National University, Daegu, Korea

S. Chang, D.H. Kim, G.N. Kim, D.J. Kong, H. Park, S.R. Ro, D.C. Son, T. Son

Chonnam National University, Institute for Universe and Elementary Particles, Kwangju, Korea

J.Y. Kim, Zero J. Kim, S. Song

Korea University, Seoul, Korea

S. Choi, D. Gyun, B. Hong, M. Jo, H. Kim, T.J. Kim, K.S. Lee, D.H. Moon, S.K. Park

University of Seoul, Seoul, Korea

M. Choi, J.H. Kim, C. Park, I.C. Park, S. Park, G. Ryu

Sungkyunkwan University, Suwon, Korea

Y. Cho, Y. Choi, Y.K. Choi, J. Goh, M.S. Kim, E. Kwon, B. Lee, J. Lee, S. Lee, H. Seo, I. Yu

Vilnius University, Vilnius, Lithuania

M.J. Bilinskas, I. Grigelionis, M. Janulis, A. Juodagalvis

Centro de Investigacion y de Estudios Avanzados del IPN, Mexico City, Mexico

H. Castilla-Valdez, E. De La Cruz-Burelo, I. Heredia-de La Cruz, R. Lopez-Fernandez, R. Magaña Villalba, J. Martínez-Ortega, A. Sánchez-Hernández, L.M. Villasenor-Cendejas

Universidad Iberoamericana, Mexico City, Mexico

S. Carrillo Moreno, F. Vazquez Valencia

Benemerita Universidad Autonoma de Puebla, Puebla, Mexico

H.A. Salazar Ibarguen

Universidad Autónoma de San Luis Potosí, San Luis Potosí, Mexico

E. Casimiro Linares, A. Morelos Pineda, M.A. Reyes-Santos

University of Auckland, Auckland, New Zealand

D. Kofcheck

University of Canterbury, Christchurch, New Zealand

A.J. Bell, P.H. Butler, R. Doesburg, S. Reucroft, H. Silverwood

National Centre for Physics, Quaid-I-Azam University, Islamabad, Pakistan

M. Ahmad, M.I. Asghar, H.R. Hoorani, S. Khalid, W.A. Khan, T. Khurshid, S. Qazi, M.A. Shah, M. Shoaib

Institute of Experimental Physics, Faculty of Physics, University of Warsaw, Warsaw, Poland

G. Brona, K. Bunkowski, M. Cwiok, W. Dominik, K. Doroba, A. Kalinowski, M. Konecki, J. Krolikowski

Soltan Institute for Nuclear Studies, Warsaw, Poland

H. Bialkowska, B. Boimska, T. Frueboes, R. Gokieli, M. Górski, M. Kazana, K. Nawrocki, K. Romanowska-Rybinska, M. Szleper, G. Wrochna, P. Zalewski

Laboratório de Instrumentação e Física Experimental de Partículas, Lisboa, Portugal

N. Almeida, P. Bargassa, A. David, P. Faccioli, M. Fernandes, P.G. Ferreira Parracho, M. Gallinaro, J. Seixas, J. Varela, P. Vischia

Joint Institute for Nuclear Research, Dubna, Russia

I. Belotelov, P. Bunin, I. Golutvin, I. Gorbunov, V. Karjavin, V. Konoplyanikov, G. Kozlov, A. Lanev, A. Malakhov, P. Moisenz, V. Palichik, V. Perelygin, M. Savina, S. Shmatov, V. Smirnov, A. Volodko, A. Zarubin

Petersburg Nuclear Physics Institute, Gatchina (St Petersburg), Russia

S. Evstyukhin, V. Golovtsov, Y. Ivanov, V. Kim, P. Levchenko, V. Murzin, V. Oreshkin, I. Smirnov, V. Sulimov, L. Uvarov, S. Vavilov, A. Vorobyev, An. Vorobyev

Institute for Nuclear Research, Moscow, Russia

Yu. Andreev, A. Dermenev, S. Gninenko, N. Golubev, M. Kirsanov, N. Krasnikov, V. Matveev, A. Pashenkov, D. Tlisov, A. Toropin

Institute for Theoretical and Experimental Physics, Moscow, Russia

V. Epshteyn, M. Erofeeva, V. Gavrilov, M. Kossov⁵, N. Lychkovskaya, V. Popov, G. Safronov, S. Semenov, V. Stolin, E. Vlasov, A. Zhokin

Moscow State University, Moscow, Russia

A. Belyaev, E. Boos, M. Dubinin⁴, L. Dudko, A. Ershov, A. Gribushin, V. Klyukhin, O. Kodolova, I. Loktin, A. Markina, S. Obraztsov, M. Perfilov, S. Petrushanko, A. Popov, L. Sarycheva[†], V. Savrin, A. Snigirev

P.N. Lebedev Physical Institute, Moscow, Russia

V. Andreev, M. Azarkin, I. Dremin, M. Kirakosyan, A. Leonidov, G. Mesyats, S.V. Rusakov, A. Vinogradov

State Research Center of Russian Federation, Institute for High Energy Physics, Protvino, Russia

I. Azhgirey, I. Bayshev, S. Bitioukov, V. Grishin⁵, V. Kachanov, D. Konstantinov, A. Korablev, V. Krychkine, V. Petrov, R. Ryutin, A. Sobol, L. Tourtchanovitch, S. Troshin, N. Tyurin, A. Uzunian, A. Volkov

University of Belgrade, Faculty of Physics and Vinca Institute of Nuclear Sciences, Belgrade, Serbia

P. Adzic²⁹, M. Djordjevic, M. Ekmedzic, D. Krpic²⁹, J. Milosevic

Centro de Investigaciones Energéticas Medioambientales y Tecnológicas (CIEMAT), Madrid, Spain

M. Aguilar-Benitez, J. Alcaraz Maestre, P. Arce, C. Battilana, E. Calvo, M. Cerrada, M. Chamizo

Llatas, N. Colino, B. De La Cruz, A. Delgado Peris, D. Domínguez Vázquez, C. Fernandez Bedoya, J.P. Fernández Ramos, A. Ferrando, J. Flix, M.C. Fouz, P. Garcia-Abia, O. Gonzalez Lopez, S. Goy Lopez, J.M. Hernandez, M.I. Josa, G. Merino, J. Puerta Pelayo, A. Quintario Olmeda, I. Redondo, L. Romero, J. Santaolalla, M.S. Soares, C. Willmott

Universidad Autónoma de Madrid, Madrid, Spain

C. Albajar, G. Codispoti, J.F. de Trocóniz

Universidad de Oviedo, Oviedo, Spain

H. Brun, J. Cuevas, J. Fernandez Menendez, S. Folgueras, I. Gonzalez Caballero, L. Lloret Iglesias, J. Piedra Gomez³⁰

Instituto de Física de Cantabria (IFCA), CSIC-Universidad de Cantabria, Santander, Spain

J.A. Brochero Cifuentes, I.J. Cabrillo, A. Calderon, S.H. Chuang, J. Duarte Campderros, M. Felcini³¹, M. Fernandez, G. Gomez, J. Gonzalez Sanchez, C. Jorda, A. Lopez Virto, J. Marco, R. Marco, C. Martinez Rivero, F. Matorras, F.J. Munoz Sanchez, T. Rodrigo, A.Y. Rodríguez-Marrero, A. Ruiz-Jimeno, L. Scodellaro, M. Sobron Sanudo, I. Vila, R. Vilar Cortabitarte

CERN, European Organization for Nuclear Research, Geneva, Switzerland

D. Abbaneo, E. Auffray, G. Auzinger, P. Baillon, A.H. Ball, D. Barney, J.F. Benitez, C. Bernet⁶, G. Bianchi, P. Bloch, A. Bocci, A. Bonato, C. Botta, H. Breuker, T. Camporesi, G. Cerminara, T. Christiansen, J.A. Coarasa Perez, D. D'Enterria, A. Dabrowski, A. De Roeck, S. Di Guida, M. Dobson, N. Dupont-Sagorin, A. Elliott-Peisert, B. Frisch, W. Funk, G. Georgiou, M. Giffels, D. Gigi, K. Gill, D. Giordano, M. Giunta, F. Glege, R. Gomez-Reino Garrido, P. Govoni, S. Gowdy, R. Guida, M. Hansen, P. Harris, C. Hartl, J. Harvey, B. Hegner, A. Hinzmann, V. Innocente, P. Janot, K. Kaadze, E. Karavakis, K. Kousouris, P. Lecoq, Y.-J. Lee, P. Lenzi, C. Lourenço, T. Mäki, M. Malberti, L. Malgeri, M. Mannelli, L. Masetti, F. Meijers, S. Mersi, E. Meschi, R. Moser, M.U. Mozer, M. Mulders, P. Musella, E. Nesvold, T. Orimoto, L. Orsini, E. Palencia Cortezon, E. Perez, L. Perrozzi, A. Petrilli, A. Pfeiffer, M. Pierini, M. Pimiä, D. Piparo, G. Polese, L. Quertenmont, A. Racz, W. Reece, J. Rodrigues Antunes, G. Rolandi³², T. Rommerskirchen, C. Rovelli³³, M. Rovere, H. Sakulin, F. Santanastasio, C. Schäfer, C. Schwick, I. Segoni, S. Sekmen, A. Sharma, P. Siegrist, P. Silva, M. Simon, P. Sphicas³⁴, D. Spiga, A. Tsirou, G.I. Veres¹⁸, J.R. Vlimant, H.K. Wöhri, S.D. Worm³⁵, W.D. Zeuner

Paul Scherrer Institut, Villigen, Switzerland

W. Bertl, K. Deiters, W. Erdmann, K. Gabathuler, R. Horisberger, Q. Ingram, H.C. Kaestli, S. König, D. Kotlinski, U. Langenegger, F. Meier, D. Renker, T. Rohe, J. Sibille³⁶

Institute for Particle Physics, ETH Zurich, Zurich, Switzerland

L. Bäni, P. Bortignon, M.A. Buchmann, B. Casal, N. Chanon, A. Deisher, G. Dissertori, M. Dittmar, M. Dünser, J. Eugster, K. Freudenreich, C. Grab, D. Hits, P. Lecomte, W. Lustermann, A.C. Marini, P. Martinez Ruiz del Arbol, N. Mohr, F. Moortgat, C. Nägeli³⁷, P. Nef, F. Nessi-Tedaldi, F. Pandolfi, L. Pape, F. Pauss, M. Peruzzi, F.J. Ronga, M. Rossini, L. Sala, A.K. Sanchez, A. Starodumov³⁸, B. Stieger, M. Takahashi, L. Tauscher[†], A. Thea, K. Theofilatos, D. Treille, C. Urscheler, R. Wallny, H.A. Weber, L. Wehrli

Universität Zürich, Zurich, Switzerland

E. Aguiló, C. Amsler, V. Chiochia, S. De Visscher, C. Favaro, M. Ivova Rikova, B. Millan Mejias, P. Otiougova, P. Robmann, H. Snoek, S. Tupputi, M. Verzetti

National Central University, Chung-Li, Taiwan

Y.H. Chang, K.H. Chen, C.M. Kuo, S.W. Li, W. Lin, Z.K. Liu, Y.J. Lu, D. Mekterovic, A.P. Singh, R. Volpe, S.S. Yu

National Taiwan University (NTU), Taipei, Taiwan

P. Bartalini, P. Chang, Y.H. Chang, Y.W. Chang, Y. Chao, K.F. Chen, C. Dietz, U. Grundler, W.-S. Hou, Y. Hsiung, K.Y. Kao, Y.J. Lei, R.-S. Lu, D. Majumder, E. Petrakou, X. Shi, J.G. Shiu, Y.M. Tzeng, X. Wan, M. Wang

Cukurova University, Adana, Turkey

A. Adiguzel, M.N. Bakirci³⁹, S. Cerci⁴⁰, C. Dozen, I. Dumanoglu, E. Eskut, S. Giris, G. Gokbulut, E. Gurpinar, I. Hos, E.E. Kangal, G. Karapinar⁴¹, A. Kayis Topaksu, G. Onengut, K. Ozdemir, S. Ozturk⁴², A. Polatoz, K. Sogut⁴³, D. Sunar Cerci⁴⁰, B. Tali⁴⁰, H. Topakli³⁹, L.N. Vergili, M. Vergili

Middle East Technical University, Physics Department, Ankara, Turkey

I.V. Akin, T. Aliev, B. Bilin, S. Bilmis, M. Deniz, H. Gamsizkan, A.M. Guler, K. Ocalan, A. Ozpineci, M. Serin, R. Sever, U.E. Surat, M. Yalvac, E. Yildirim, M. Zeyrek

Bogazici University, Istanbul, Turkey

E. Gürmez, B. Isildak⁴⁴, M. Kaya⁴⁵, O. Kaya⁴⁵, S. Ozkorucuklu⁴⁶, N. Sonmez⁴⁷

Istanbul Technical University, Istanbul, Turkey

K. Cankocak

National Scientific Center, Kharkov Institute of Physics and Technology, Kharkov, Ukraine

L. Levchuk

University of Bristol, Bristol, United Kingdom

F. Bostock, J.J. Brooke, E. Clement, D. Cussans, H. Flacher, R. Frazier, J. Goldstein, M. Grimes, G.P. Heath, H.F. Heath, L. Kreczko, S. Metson, D.M. Newbold³⁵, K. Nirunpong, A. Poll, S. Senkin, V.J. Smith, T. Williams

Rutherford Appleton Laboratory, Didcot, United Kingdom

L. Basso⁴⁸, K.W. Bell, A. Belyaev⁴⁸, C. Brew, R.M. Brown, D.J.A. Cockerill, J.A. Coughlan, K. Harder, S. Harper, J. Jackson, B.W. Kennedy, E. Olaiya, D. Petyt, B.C. Radburn-Smith, C.H. Shepherd-Themistocleous, I.R. Tomalin, W.J. Womersley

Imperial College, London, United Kingdom

R. Bainbridge, G. Ball, R. Beuselinck, O. Buchmuller, D. Colling, N. Cripps, M. Cutajar, P. Dauncey, G. Davies, M. Della Negra, W. Ferguson, J. Fulcher, D. Futyan, A. Gilbert, A. Guneratne Bryer, G. Hall, Z. Hatherell, J. Hays, G. Iles, M. Jarvis, G. Karapostoli, L. Lyons, A.-M. Magnan, J. Marrouche, B. Mathias, R. Nandi, J. Nash, A. Nikitenko³⁸, A. Papageorgiou, J. Pela⁵, M. Pesaresi, K. Petridis, M. Pioppi⁴⁹, D.M. Raymond, S. Rogerson, A. Rose, M.J. Ryan, C. Seez, P. Sharp[†], A. Sparrow, M. Stoye, A. Tapper, M. Vazquez Acosta, T. Virdee, S. Wakefield, N. Wardle, T. Whyntie

Brunel University, Uxbridge, United Kingdom

M. Chadwick, J.E. Cole, P.R. Hobson, A. Khan, P. Kyberd, D. Leggat, D. Leslie, W. Martin, I.D. Reid, P. Symonds, L. Teodorescu, M. Turner

Baylor University, Waco, USA

K. Hatakeyama, H. Liu, T. Scarborough

The University of Alabama, Tuscaloosa, USA

O. Charaf, C. Henderson, P. Rumerio

Boston University, Boston, USA

A. Avetisyan, T. Bose, C. Fantasia, A. Heister, J. St. John, P. Lawson, D. Lazic, J. Rohlf, D. Sperka, L. Sulak

Brown University, Providence, USA

J. Alimena, S. Bhattacharya, D. Cutts, A. Ferapontov, U. Heintz, S. Jabeen, G. Kukartsev, E. Laird, G. Landsberg, M. Luk, M. Narain, D. Nguyen, M. Segala, T. Sinthuprasith, T. Speer, K.V. Tsang

University of California, Davis, Davis, USA

R. Breedon, G. Breto, M. Calderon De La Barca Sanchez, S. Chauhan, M. Chertok, J. Conway, R. Conway, P.T. Cox, J. Dolen, R. Erbacher, M. Gardner, R. Houtz, W. Ko, A. Kopecky, R. Lander, T. Miceli, D. Pellett, B. Rutherford, M. Searle, J. Smith, M. Squires, M. Tripathi, R. Vasquez Sierra

University of California, Los Angeles, Los Angeles, USA

V. Andreev, D. Cline, R. Cousins, J. Duris, S. Erhan, P. Everaerts, C. Farrell, J. Hauser, M. Ignatenko, C. Jarvis, C. Plager, G. Rakness, P. Schlein[†], J. Tucker, V. Valuev, M. Weber

University of California, Riverside, Riverside, USA

J. Babb, R. Clare, M.E. Dinardo, J. Ellison, J.W. Gary, F. Giordano, G. Hanson, G.Y. Jeng⁵⁰, H. Liu, O.R. Long, A. Luthra, H. Nguyen, S. Paramesvaran, J. Sturdy, S. Sumowidagdo, R. Wilken, S. Wimpenny

University of California, San Diego, La Jolla, USA

W. Andrews, J.G. Branson, G.B. Cerati, S. Cittolin, D. Evans, F. Golf, A. Holzner, R. Kelley, M. Lebourgeois, J. Letts, I. Macneill, B. Mangano, S. Padhi, C. Palmer, G. Petrucciani, M. Pieri, M. Sani, V. Sharma, S. Simon, E. Sudano, M. Tadel, Y. Tu, A. Vartak, S. Wasserbaech⁵¹, F. Würthwein, A. Yagil, J. Yoo

University of California, Santa Barbara, Santa Barbara, USA

D. Barge, R. Bellan, C. Campagnari, M. D'Alfonso, T. Danielson, K. Flowers, P. Geffert, J. Incandela, C. Justus, P. Kalavase, S.A. Koay, D. Kovalskyi, V. Krutelyov, S. Lowette, N. Mccoll, V. Pavlunin, F. Rebassoo, J. Ribnik, J. Richman, R. Rossin, D. Stuart, W. To, C. West

California Institute of Technology, Pasadena, USA

A. Apresyan, A. Bornheim, Y. Chen, E. Di Marco, J. Duarte, M. Gataullin, Y. Ma, A. Mott, H.B. Newman, C. Rogan, M. Spiropulu⁴, V. Timciuc, P. Traczyk, J. Veverka, R. Wilkinson, Y. Yang, R.Y. Zhu

Carnegie Mellon University, Pittsburgh, USA

B. Akgun, R. Carroll, T. Ferguson, Y. Iiyama, D.W. Jang, Y.F. Liu, M. Paulini, H. Vogel, I. Vorobiev

University of Colorado at Boulder, Boulder, USA

J.P. Cumalat, B.R. Drell, C.J. Edelmaier, W.T. Ford, A. Gaz, B. Heyburn, E. Luiggi Lopez, J.G. Smith, K. Stenson, K.A. Ulmer, S.R. Wagner

Cornell University, Ithaca, USA

J. Alexander, A. Chatterjee, N. Eggert, L.K. Gibbons, B. Heltsley, A. Khukhunaishvili, B. Kreis, N. Mirman, G. Nicolas Kaufman, J.R. Patterson, A. Ryd, E. Salvati, W. Sun, W.D. Teo, J. Thom, J. Thompson, J. Vaughan, Y. Weng, L. Winstrom, P. Wittich

Fairfield University, Fairfield, USA

D. Winn

Fermi National Accelerator Laboratory, Batavia, USA

S. Abdullin, M. Albrow, J. Anderson, L.A.T. Bauerdick, A. Beretvas, J. Berryhill, P.C. Bhat, I. Bloch, K. Burkett, J.N. Butler, V. Chetluru, H.W.K. Cheung, F. Chlebana, V.D. Elvira, I. Fisk, J. Freeman, Y. Gao, D. Green, O. Gutsche, J. Hanlon, R.M. Harris, J. Hirschauer, B. Hooberman, S. Jindariani, M. Johnson, U. Joshi, B. Kilminster, B. Klima, S. Kunori, S. Kwan, C. Leonidopoulos, D. Lincoln, R. Lipton, J. Lykken, K. Maeshima, J.M. Marraffino, S. Maruyama, D. Mason, P. McBride, K. Mishra, S. Mrenna, Y. Musienko⁵², C. Newman-Holmes, V. O'Dell, O. Prokofyev, E. Sexton-Kennedy, S. Sharma, W.J. Spalding, L. Spiegel, P. Tan, L. Taylor, S. Tkaczyk, N.V. Tran, L. Uplegger, E.W. Vaandering, R. Vidal, J. Whitmore, W. Wu, F. Yang, F. Yumiceva, J.C. Yun

University of Florida, Gainesville, USA

D. Acosta, P. Avery, D. Bourilkov, M. Chen, S. Das, M. De Gruttola, G.P. Di Giovanni, D. Dobur, A. Drozdetskiy, R.D. Field, M. Fisher, Y. Fu, I.K. Furic, J. Gartner, J. Hugon, B. Kim, J. Konigsberg, A. Korytov, A. Kropivnitskaya, T. Kypreos, J.F. Low, K. Matchev, P. Milenovic⁵³, G. Mitselmakher, L. Muniz, R. Remington, A. Rinkevicius, P. Sellers, N. Skhirtladze, M. Snowball, J. Yelton, M. Zakaria

Florida International University, Miami, USA

V. Gaultney, L.M. Lebolo, S. Linn, P. Markowitz, G. Martinez, J.L. Rodriguez

Florida State University, Tallahassee, USA

J.R. Adams, T. Adams, A. Askew, J. Bochenek, J. Chen, B. Diamond, S.V. Gleyzer, J. Haas, S. Hagopian, V. Hagopian, M. Jenkins, K.F. Johnson, H. Prosper, V. Veeraraghavan, M. Weinberg

Florida Institute of Technology, Melbourne, USA

M.M. Baarmann, B. Dorney, M. Hohlmann, H. Kalakhety, I. Vodopiyanov

University of Illinois at Chicago (UIC), Chicago, USA

M.R. Adams, I.M. Anghel, L. Apanasevich, Y. Bai, V.E. Bazterra, R.R. Betts, I. Bucinskaite, J. Callner, R. Cavanaugh, C. Dragoiu, O. Evdokimov, L. Gauthier, C.E. Gerber, D.J. Hofman, S. Khalatyan, F. Lacroix, M. Malek, C. O'Brien, C. Silkworth, D. Strom, N. Varelas

The University of Iowa, Iowa City, USA

U. Akgun, E.A. Albayrak, B. Bilki⁵⁴, W. Clarida, F. Duru, S. Griffiths, J.-P. Merlo, H. Mermerkaya⁵⁵, A. Mestvirishvili, A. Moeller, J. Nachtman, C.R. Newsom, E. Norbeck, Y. Onel, F. Ozok, S. Sen, E. Tiras, J. Wetzel, T. Yetkin, K. Yi

Johns Hopkins University, Baltimore, USA

B.A. Barnett, B. Blumenfeld, S. Bolognesi, D. Fehling, G. Giurgiu, A.V. Gritsan, Z.J. Guo, G. Hu, P. Maksimovic, S. Rappoccio, M. Swartz, A. Whitbeck

The University of Kansas, Lawrence, USA

P. Baringer, A. Bean, G. Benelli, O. Grachov, R.P. Kenny Iii, M. Murray, D. Noonan, S. Sanders, R. Stringer, G. Tinti, J.S. Wood, V. Zhukova

Kansas State University, Manhattan, USA

A.F. Barfuss, T. Bolton, I. Chakaberia, A. Ivanov, S. Khalil, M. Makouski, Y. Maravin, S. Shrestha, I. Svintradze

Lawrence Livermore National Laboratory, Livermore, USA

J. Gronberg, D. Lange, D. Wright

University of Maryland, College Park, USA

A. Baden, M. Boutemeur, B. Calvert, S.C. Eno, J.A. Gomez, N.J. Hadley, R.G. Kellogg, M. Kirn,

T. Kolberg, Y. Lu, M. Marionneau, A.C. Mignerey, K. Pedro, A. Peterman, A. Skuja, J. Temple, M.B. Tonjes, S.C. Tonwar, E. Twedt

Massachusetts Institute of Technology, Cambridge, USA

A. Apyan, G. Bauer, J. Bendavid, W. Busza, E. Butz, I.A. Cali, M. Chan, V. Dutta, G. Gomez Ceballos, M. Goncharov, K.A. Hahn, Y. Kim, M. Klute, K. Krajczar⁵⁶, W. Li, P.D. Luckey, T. Ma, S. Nahn, C. Paus, D. Ralph, C. Roland, G. Roland, M. Rudolph, G.S.F. Stephans, F. Stöckli, K. Sumorok, K. Sung, D. Velicanu, E.A. Wenger, R. Wolf, B. Wyslouch, S. Xie, M. Yang, Y. Yilmaz, A.S. Yoon, M. Zanetti

University of Minnesota, Minneapolis, USA

S.I. Cooper, B. Dahmes, A. De Benedetti, G. Franzoni, A. Gude, S.C. Kao, K. Klapoetke, Y. Kubota, J. Mans, N. Pastika, R. Rusack, M. Sasseville, A. Singovsky, N. Tambe, J. Turkewitz

University of Mississippi, University, USA

L.M. Cremaldi, R. Kroeger, L. Perera, R. Rahmat, D.A. Sanders

University of Nebraska-Lincoln, Lincoln, USA

E. Avdeeva, K. Bloom, S. Bose, J. Butt, D.R. Claes, A. Dominguez, M. Eads, J. Keller, I. Kravchenko, J. Lazo-Flores, H. Malbouisson, S. Malik, G.R. Snow

State University of New York at Buffalo, Buffalo, USA

U. Baur, A. Godshalk, I. Iashvili, S. Jain, A. Kharchilava, A. Kumar, S.P. Shipkowski, K. Smith

Northeastern University, Boston, USA

G. Alverson, E. Barberis, D. Baumgartel, M. Chasco, J. Haley, D. Nash, D. Trocino, D. Wood, J. Zhang

Northwestern University, Evanston, USA

A. Anastassov, A. Kubik, N. Mucia, N. Odell, R.A. Ofierzynski, B. Pollack, A. Pozdnyakov, M. Schmitt, S. Stoynev, M. Velasco, S. Won

University of Notre Dame, Notre Dame, USA

L. Antonelli, D. Berry, A. Brinkerhoff, M. Hildreth, C. Jessop, D.J. Karmgard, J. Kolb, K. Lannon, W. Luo, S. Lynch, N. Marinelli, D.M. Morse, T. Pearson, R. Ruchti, J. Slaunwhite, N. Valls, M. Wayne, M. Wolf

The Ohio State University, Columbus, USA

B. Bylsma, L.S. Durkin, A. Hart, C. Hill, R. Hughes, K. Kotov, T.Y. Ling, D. Puigh, M. Rodenburg, C. Vuosalo, G. Williams, B.L. Winer

Princeton University, Princeton, USA

N. Adam, E. Berry, P. Elmer, D. Gerbaudo, V. Halyo, P. Hebda, J. Hegeman, A. Hunt, P. Jindal, D. Lopes Pegna, P. Lujan, D. Marlow, T. Medvedeva, M. Mooney, J. Olsen, P. Piroué, X. Quan, A. Raval, B. Safdi, H. Saka, D. Stickland, C. Tully, J.S. Werner, A. Zuranski

University of Puerto Rico, Mayaguez, USA

J.G. Acosta, E. Brownson, X.T. Huang, A. Lopez, H. Mendez, S. Oliveros, J.E. Ramirez Vargas, A. Zatserklyaniy

Purdue University, West Lafayette, USA

E. Alagoz, V.E. Barnes, D. Benedetti, G. Bolla, D. Bortoletto, M. De Mattia, A. Everett, Z. Hu, M. Jones, O. Koybasi, M. Kress, A.T. Laasanen, N. Leonardo, V. Maroussov, P. Merkel, D.H. Miller, N. Neumeister, I. Shipsey, D. Silvers, A. Svyatkovskiy, M. Vidal Marono, H.D. Yoo, J. Zablocki, Y. Zheng

Purdue University Calumet, Hammond, USA

S. Guragain, N. Parashar

Rice University, Houston, USA

A. Adair, C. Boulahouache, K.M. Ecklund, F.J.M. Geurts, B.P. Padley, R. Redjimi, J. Roberts, J. Zabel

University of Rochester, Rochester, USA

B. Betchart, A. Bodek, Y.S. Chung, R. Covarelli, P. de Barbaro, R. Demina, Y. Eshaq, A. Garcia-Bellido, P. Goldenzweig, J. Han, A. Harel, D.C. Miner, D. Vishnevskiy, M. Zielinski

The Rockefeller University, New York, USA

A. Bhatti, R. Ciesielski, L. Demortier, K. Goulianatos, G. Lungu, S. Malik, C. Mesropian

Rutgers, the State University of New Jersey, Piscataway, USA

S. Arora, A. Barker, J.P. Chou, C. Contreras-Campana, E. Contreras-Campana, D. Duggan, D. Ferencek, Y. Gershtein, R. Gray, E. Halkiadakis, D. Hidas, A. Lath, S. Panwalkar, M. Park, R. Patel, V. Rekovic, J. Robles, K. Rose, S. Salur, S. Schnetzer, C. Seitz, S. Somalwar, R. Stone, S. Thomas

University of Tennessee, Knoxville, USA

G. Cerizza, M. Hollingsworth, S. Spanier, Z.C. Yang, A. York

Texas A&M University, College Station, USA

R. Eusebi, W. Flanagan, J. Gilmore, T. Kamon⁵⁷, V. Khotilovich, R. Montalvo, I. Osipenkov, Y. Pakhotin, A. Perloff, J. Roe, A. Safonov, T. Sakuma, S. Sengupta, I. Suarez, A. Tatarinov, D. Toback

Texas Tech University, Lubbock, USA

N. Akchurin, J. Damgov, P.R. Dudero, C. Jeong, K. Kovitanggoon, S.W. Lee, T. Libeiro, Y. Roh, I. Volobouev

Vanderbilt University, Nashville, USA

E. Appelt, C. Florez, S. Greene, A. Gurrola, W. Johns, C. Johnston, P. Kurt, C. Maguire, A. Melo, P. Sheldon, B. Snook, S. Tuo, J. Velkovska

University of Virginia, Charlottesville, USA

M.W. Arenton, M. Balazs, S. Boutle, B. Cox, B. Francis, J. Goodell, R. Hirosky, A. Ledovskoy, C. Lin, C. Neu, J. Wood, R. Yohay

Wayne State University, Detroit, USA

S. Gollapinni, R. Harr, P.E. Karchin, C. Kottachchi Kankanamge Don, P. Lamichhane, A. Sakharov

University of Wisconsin, Madison, USA

M. Anderson, M. Bachtis, D. Belknap, L. Borrello, D. Carlsmith, M. Cepeda, S. Dasu, L. Gray, K.S. Grogg, M. Grothe, R. Hall-Wilton, M. Herndon, A. Hervé, P. Klabbers, J. Klukas, A. Lanaro, C. Lazaridis, J. Leonard, R. Loveless, A. Mohapatra, I. Ojalvo, F. Palmonari, G.A. Pierro, I. Ross, A. Savin, W.H. Smith, J. Swanson

†: Deceased

1: Also at Vienna University of Technology, Vienna, Austria

2: Also at National Institute of Chemical Physics and Biophysics, Tallinn, Estonia

3: Also at Universidade Federal do ABC, Santo Andre, Brazil

4: Also at California Institute of Technology, Pasadena, USA

- 5: Also at CERN, European Organization for Nuclear Research, Geneva, Switzerland
- 6: Also at Laboratoire Leprince-Ringuet, Ecole Polytechnique, IN2P3-CNRS, Palaiseau, France
- 7: Also at Suez Canal University, Suez, Egypt
- 8: Also at Zewail City of Science and Technology, Zewail, Egypt
- 9: Also at Cairo University, Cairo, Egypt
- 10: Also at Fayoum University, El-Fayoum, Egypt
- 11: Also at British University, Cairo, Egypt
- 12: Now at Ain Shams University, Cairo, Egypt
- 13: Also at Soltan Institute for Nuclear Studies, Warsaw, Poland
- 14: Also at Université de Haute-Alsace, Mulhouse, France
- 15: Also at Moscow State University, Moscow, Russia
- 16: Also at Brandenburg University of Technology, Cottbus, Germany
- 17: Also at Institute of Nuclear Research ATOMKI, Debrecen, Hungary
- 18: Also at Eötvös Loránd University, Budapest, Hungary
- 19: Also at Tata Institute of Fundamental Research - HECR, Mumbai, India
- 20: Also at University of Visva-Bharati, Santiniketan, India
- 21: Also at Sharif University of Technology, Tehran, Iran
- 22: Also at Isfahan University of Technology, Isfahan, Iran
- 23: Also at Plasma Physics Research Center, Science and Research Branch, Islamic Azad University, Teheran, Iran
- 24: Also at Facoltà Ingegneria Università di Roma, Roma, Italy
- 25: Also at Università della Basilicata, Potenza, Italy
- 26: Also at Università degli Studi Guglielmo Marconi, Roma, Italy
- 27: Also at Università degli studi di Siena, Siena, Italy
- 28: Also at University of Bucharest, Faculty of Physics, Bucuresti-Magurele, Romania
- 29: Also at Faculty of Physics of University of Belgrade, Belgrade, Serbia
- 30: Also at University of Florida, Gainesville, USA
- 31: Also at University of California, Los Angeles, Los Angeles, USA
- 32: Also at Scuola Normale e Sezione dell' INFN, Pisa, Italy
- 33: Also at INFN Sezione di Roma; Università di Roma "La Sapienza", Roma, Italy
- 34: Also at University of Athens, Athens, Greece
- 35: Also at Rutherford Appleton Laboratory, Didcot, United Kingdom
- 36: Also at The University of Kansas, Lawrence, USA
- 37: Also at Paul Scherrer Institut, Villigen, Switzerland
- 38: Also at Institute for Theoretical and Experimental Physics, Moscow, Russia
- 39: Also at Gaziosmanpasa University, Tokat, Turkey
- 40: Also at Adiyaman University, Adiyaman, Turkey
- 41: Also at Izmir Institute of Technology, Izmir, Turkey
- 42: Also at The University of Iowa, Iowa City, USA
- 43: Also at Mersin University, Mersin, Turkey
- 44: Also at Ozyegin University, Istanbul, Turkey
- 45: Also at Kafkas University, Kars, Turkey
- 46: Also at Suleyman Demirel University, Isparta, Turkey
- 47: Also at Ege University, Izmir, Turkey
- 48: Also at School of Physics and Astronomy, University of Southampton, Southampton, United Kingdom
- 49: Also at INFN Sezione di Perugia; Università di Perugia, Perugia, Italy
- 50: Also at University of Sydney, Sydney, Australia
- 51: Also at Utah Valley University, Orem, USA

- 52: Also at Institute for Nuclear Research, Moscow, Russia
- 53: Also at University of Belgrade, Faculty of Physics and Vinca Institute of Nuclear Sciences, Belgrade, Serbia
- 54: Also at Argonne National Laboratory, Argonne, USA
- 55: Also at Erzincan University, Erzincan, Turkey
- 56: Also at KFKI Research Institute for Particle and Nuclear Physics, Budapest, Hungary
- 57: Also at Kyungpook National University, Daegu, Korea